Wave Blocking Phenomena and Ecological Applications

James Dowdall

Thesis submitted to the Faculty of Graduate and Postdoctoral Studies in partial fulfillment of the requirements for the degree of
Master of Science in Mathematics [1]

Department of Mathematics and Statistics
Faculty of Science
University of Ottawa

[1] The M.Sc. program is a joint program with Carleton University, administered by the Ottawa-Carleton Institute of Mathematics and Statistics

Abstract

The growing flow of people and goods around the globe has allowed new, non-native species to establish and spread in already fragile ecosystems. The introduction of invasive species can have a detrimental impact on the already established species. Thus, it is important that we understand the mechanisms that facilitate or prevent invasion. Since reaction-diffusion invasion models produce travelling waves we can study invasion by looking at the mechanisms that allow for wave propagation failure, or wave-blocking. In this thesis we consider a perturbed reaction-diffusion model in which the perturbation resides in either the reaction or diffusion term. In doing so we exploit the underlying symmetry of our problem to define a region in the appropriate parameter space that leads to wave blocking. As a demonstrative example we apply our theory to the bistable equation and consider the effects of various perturbations.

Acknowledgements

The completion of a thesis or dissertation is by no means a simple task. Throughout the past two years I have received support and help from an incredible number of people. In particular, I'd like to thank my supervisors, Dr. Victor LeBlanc and Dr. Frithjof Lutscher, for their continued guidance and support. I can never thank them enough for all the time they have invested in me and for teaching me so much throughout my masters. I also want to express my gratitude to the University of Ottawa for this incredible opportunity. Finally, last but not least, I'd like to thank my family and friends who have been there every step of the way.

Dedication

This work is dedicated to my parents. Despite the distance, they have always been there supporting and encouraging me. I wouldn't be where and who I am without them. I'm proud to be their son.

Contents

List of Figures **vii**

1 Introduction **1**

1.1 Travelling Waves 1

1.2 Habitat Fragmentation 3

1.3 The Gap Model 5

1.4 The Problem 6

2 Ecological Phenomena **9**

2.1 Ecological Framework 9

2.2 Homogenization 10

2.2.1 The $O(l^{-2})$ Equation 12

2.2.2 The $O(l^{-1})$ Equation 12

2.2.3 The $O(l^{0})$ Equation 13

2.3 Homogenization and Invasion Pinning 14

3 Wave Blocking Phenomena **18**

3.1 Setup 19

3.2 Relative Equilibria and Wave Speed 21

3.3 The Linear Operator L 22

3.4 The Centre Manifold 24

3.5 Wave-Blocking in the Perturbed System 27

4 Numerical Results **33**

4.1 Numerical Setup 33

4.2 Example 1: Perturbation In The Reaction Term 35

4.3 Example 2: Perturbation In The Diffusion Term 36

4.4 Example 3: Ecological Diffusion 39

4.5 Example 4: Spatial Correlation 41

5 Conclusion **46**

A MATLAB Code **49**

A.1 Numerical Calculation of $r(a)$ 49

A.2 Wedge Plotting Program 51

Bibliography **56**

List of Figures

1.1 Visual representations of the diffusion coefficient $D(x)$ as considered by Lewis & Keener, Shigesada et al ([18] Fig. 1. pp. 145) . and Kinezaki et al. ([8] Fig. 1. pp. 264). 7

1.2 The cone of parameter values in (c, ε) parameter space that leads to propagation failure [11, 16]. 8

2.1 Plot of the homogenized speed c_{approx} as a function of the parameter B for fixed values of $A = 1, 2, 3, 4$ and $\alpha = 0.4646$. 17

2.2 Evolution of a travelling wave solution of equation (2.2.1) with (2.3.1), $D(x) = 1 + B\sin(x)$, $\alpha(x) = \alpha$ and $\rho(x) = 1$. The initial wave profile is given by a solid line while the successive snapshots taken at regular time intervals, are given by the dashed lines. Parameters are $\alpha = 0.4646$, and $B = 0.1$ (left), $B = 0.35$ (right) . . . 17

3.1 The relative equilibria on the unperturbed manifold ([11] Figure 2 p. 25). 26

3.2 The perturbed equilibrium on the manifold $\mathcal{S}_\varepsilon$. The curve Θ_ε corresponds to the set of blocking points and is given by $a_t = 0$. ([11] Figure 3 p. 26). 31

3.3 Wave-blocking occurs for values of (ε, c) inside the wedge. Here r_{max} and r_{min} are the supremum and infimum of (3.5.8) respectively. . . . 32

4.1 A visualization of the scheme used to numerically obtain the initial blocking values. 34
4.2 Plot of $p(x)$ (solid blue line with circles) and $P(x)$ (solid red line) with $n = 13$. 36
4.3 Plot of $r(a)$ for $\mathcal{G}$ given by (4.2.1). 37
4.4 Comparison between the blocking wedge (line) and the numerically calculated values of wave-blocking (stars) for the perturbation corresponding to (4.2.1) 38
4.5 Comparison between the blocking wedge (line) and the numerically calculated values of wave-blocking (stars) for (4.3.1). 39
4.6 Comparison between the blocking wedge (line) and the numerically calculated values of wave-blocking (stars) for the perturbation in (4.4.1). 41
4.7 Plot of $\sup\{r(a)\}$ as a function of $\boldsymbol{\theta}$ for equation (4.5.1) (Top) and (4.5.2) (Bottom). 42
4.8 Plot of $\rho(x)$ (dashed red line) and $D(x)$ (solid blue line) for $\varepsilon = 0.25$ and $\boldsymbol{\theta} = 0$. The arrows indicate the direction of the movement bias. 45

Chapter 1

Introduction

1.1 Travelling Waves

An essential component in the study of linear and nonlinear partial differential equations is the phenomenon of wave propagation. Wave propagation is of fundamental importance in the study of a diverse set of problems in fields ranging from physics and chemistry to biology [21]. The mathematical theory of travelling waves extends to integrodifference equations, integrodifferential equations, etc., but is most fully developed in the context of partial differential equations.

Reaction-Diffusion equations (RDEs) are among the primary mathematical tools used in studying biological invasions. Furthermore, RDEs are natural candidates when it comes to studying travelling waves. Traditionally, RDEs take the form

$$\frac{\partial u}{\partial t} = D\Delta u + \mathcal{F}(u) \tag{1.1.1}$$

where $u(t, x)$ is a vector whose components represent the concentration of some substance at time $t \in \mathbb{R}^+$ and at $x \in \mathbb{R}^N$. The term $D\Delta u$ is often referred to as the diffusion term as it represents the observed diffusive behaviours and the diffusion coefficient D measures the dispersal rate. The second term, $\mathcal{F}(u)$, is the reaction term.

It accounts for all local reactions that are specific to the situation being studied. For example, in ecology, the reaction term describes population growth dynamics.

Now that we have equation (1.1.1) we need to formally define what it means for a solution of (1.1.1) to be a travelling wave. When $N = 1$ we define a travelling wave to be a solution $u(t, x)$ such that $u(t, x) = w(x + ct)$ where w is some function of the variable $\eta = x + ct$ and c is a constant (speed of the wave). Thus, the function $w(\eta)$ must satisfy the differential equation

$$cw' = Dw'' + \mathcal{F}(w). \tag{1.1.2}$$

However, not all solutions of (1.1.2) are of interest. A wave front is characterized by

$$\lim_{\eta\to\pm\infty} w(\eta) = w_{\pm}, \qquad \lim_{\eta\to\pm\infty} w'(\eta) = 0, \tag{1.1.3}$$

assuming the limits exist and that $w_+ \neq w_-$. Rewriting equation (1.1.2) as a system of ODE's gives us

$$\begin{cases} w' = v, \\ v' = \frac{1}{D}\left[cv - \mathcal{F}(w)\right]. \end{cases} \tag{1.1.4}$$

We know that a travelling wave solution has different limits as $\eta \to \pm\infty$ which can be represented by a heteroclinic orbit of (1.1.4). In order to find these orbits we need to look at the equilibrium points. It can be seen that the equilibrium points of (1.1.4) are of the form $(0, w)$ where $\mathcal{F}(w) = 0$. Thus, $w_{\pm}$ are equilibrium points of the non spatial system [21]

$$\frac{du}{dt} = \mathcal{F}(u).$$

It is natural to ask if systems such as (1.1.1) possess travelling wave solutions. Furthermore, do those solutions exist for every value of c? It turns out that the existence of travelling waves depends on the stability of the stationary points $w_{\pm}$. There are three possibilities;

(i) Both stationary points are stable (Bistable).

(ii) One of the points is stable and the other is unstable (Monostable).

(iii) Both points are unstable.

For the bistable case, we have the following theorem that guarantees the existence of a travelling wave.

Theorem 1.1.1. *([21] Theorem 2.1 pp. 15.) Let $\mathcal{F}(u)$ vanish at a finite number of points u_n, $w_+ \leq u_n \leq w_-$ $(n = 1,....,k)$. Let us assume that $\mathcal{F}'(w_\pm) < 0$ and that $\mathcal{F}'(u_n) > 0$ for at least one point where $\mathcal{F}$ vanishes. Then there exists a unique monotone traveling wave, i.e., a constant c and a twice differentiable function $w(x)$ satisfying* (1.1.2) *and* (1.1.3).

Consider the bistable equation

$$\frac{\partial u}{\partial t} = \frac{\partial^2 u}{\partial x^2} + u(1-u)(u-\alpha) \tag{1.1.5}$$

where $\alpha \in (0,1)$ is a real parameter. The cubic nonlinearity satisfies the conditions of theorem 1.1.1, it is therefore expected that we can find a travelling wave solution. It has been shown using phase plane analysis that (1.1.5) has a travelling wave solution of the form [6]

$$u(t,x) = \frac{1}{2}\left(1 + \tanh\left(\frac{x + ct + K}{2\sqrt{2}}\right)\right) \tag{1.1.6}$$

where K is any real constant. Furthermore, the unique wave speed is given by [6, 7, 12]

$$c = \frac{1}{\sqrt{2}}(1 - 2\alpha). \tag{1.1.7}$$

1.2 Habitat Fragmentation

Diffusion models such as (1.1.1) often view space as a homogeneous continuum. In an ecological setting this assumption is rarely, if ever, true [7]. Natural environments are becoming more and more fragmented as a result of natural causes and human

intervention. Spatial variation in habitats can imperil the persistence of native species and it may provide more opportunities for alien species to invade and take over.

The study of reaction-diffusion equations in highly fragmented environments dates back to the work of Shigesada et al [9, 18]. They considered a heterogeneous environment that consisted of two patch types, a favourable patch of length l_1 and an unfavourable patch of length l_2, which are arranged periodically in an infinitely long habitat. The population dynamics are governed by the generalized Fisher equation,

$$\frac{\partial u}{\partial t} = \frac{\partial}{\partial x}\left[D(x)\frac{\partial u}{\partial x}\right] + (\rho(x) - \mu u)u, \tag{1.2.1}$$

where $\rho(x)$ is the intrinsic growth rate and $\mu > 0$ is a coefficient that represents the competition between members of the same species. The functions $D(x)$ and $\rho(x)$ are taken to be periodic step functions (see Figure 1.1)

$$D(x) = \begin{cases} D_1 & \text{in patch type 1,} \\ D_2 & \text{in patch type 2,} \end{cases} \qquad \rho(x) = \begin{cases} \rho_1 & \text{in patch type 1,} \\ \rho_2 & \text{in patch type 2.} \end{cases}$$

Furthermore, the authors of [18] imposed conditions at the boundaries of two patches which guaranteed the continuity of the density and flux. Shigesada et al. [18] noticed that there existed a minimal positive time t^* for which $u(t, x) = u(t + t^*, x + l)$ where $l = l_1 + l_2$ (i.e, the spatial period). An advancing wave front satisfying this condition is called a travelling periodic wave (TPW). At the time of their publication, Shigesada et al. did not prove the existence or stability of the TPW but instead derived an implicit function for the speed of the propagating wave front $c = l/t^*$. Furthermore, the speed of the propagating wave is approximated by $2\sqrt{\langle\rho(x)\rangle_A\langle D(x)\rangle_H}$ when the patch widths are sufficiently small. Here $\langle\rho(x)\rangle_A$ is the arithmetic mean of $\rho(x)$, and $\langle D(x)\rangle_H$ is the harmonic mean of $D(x)$, respectively defined by

$$\langle\rho(x)\rangle_A = \frac{1}{2l}\int_{-l}^{l}\rho(x)\,dx,$$

$$\langle D(x)\rangle_H = \left[\frac{1}{2l}\int_{-l}^{l}\frac{1}{D(x)}\,dx\right]^{-1}.$$

On the basis of this work Kinezaki et al. [8] considered an environment in which the coefficient functions vary sinusoidally in space. In contrast to the patch model above they sought to show how the amplitude and wavelength of the oscillations affected the rate of spread. As a case example (see Figure 1.1) the authors in [8] considered (1.2.1) with

$$\rho(x) = 1, \qquad \mu = 1, \qquad D(x) = A + B\sin(x).$$

The authors found that the speed decreases with increases in the amplitude B. In particular if $A = B$ then the speed falls to zero while the species persists in a local region surrounding the initial invasion point [8]. In this case the invasion front stalls, neither advancing nor retreating.

1.3 The Gap Model

The spatial heterogeneities that can cause an invasion front to stall leads to a phenomenom called *invasion pinning* or *wave blocking*. Early research in wave blocking phenomena centred around the bistable equation with a passive gap region or, as it is more commonly referred to, the gap model [5]. While the gap model is a simplistic model, its applications are far reaching, ranging from problems in population genetics to the study of wave propagation in cardiac tissue. The model is an RDE of the form

$$\frac{\partial u}{\partial t} = \frac{\partial}{\partial x}\left[D(x)\frac{\partial u}{\partial x}\right] + \mathcal{H}(u,x) \tag{1.3.1}$$

where

$$D(x) = \begin{cases} D, & 0, \leq x \leq l \\ 1 & \text{otherwise} \end{cases} \tag{1.3.2}$$

and

$$\mathcal{H}(u,x) = \begin{cases} g(u,x), & 0 \leq x \leq l \\ f(u), & \text{otherwise.} \end{cases} \tag{1.3.3}$$

Here l denotes the length of the gap. Furthermore, the reaction terms f and g describe the dynamics outside and inside the gap respectively.

Propagation failure, or wave blocking, for this type of local inhomogeneity was studied by J. Keener and T. Lewis. In [5] g is taken to be zero while f is given by

$$f(u) = u(1-u)(u-\alpha) \tag{1.3.4}$$

where $0 \leq \alpha \leq 1$.

The authors in [5] observed that for particular parameter values there exist different stationary solutions [5], denoted by U, which satisfy the boundary value problem

$$\begin{aligned} 0 &= \tfrac{\partial}{\partial x}\left[D(x)\tfrac{\partial U}{\partial x}\right] + \mathcal{H}(U,x), \\ U(-\infty) &= 0, \qquad U(\infty) = 1. \end{aligned} \tag{1.3.5}$$

By applying comparison principles, Lewis and Keener argued that finding conditions for wave blocking is equivalent to finding conditions for the existence of steady state solutions.

Using a geometric interpretation, Lewis and Keener showed that there exists a critical value l^* such that (1.3.5) has no solutions for $l < l^*$, one solution for $l = l^*$ and at least two solutions for $l > l^*$. Furthermore, solutions arise or disappear via a limit point bifurcation [5].

1.4 The Problem

In recent years, there has been growing interest in the phenomena of propagation failure and invasion pinning. Natural systems are constantly exposed to external stimuli that impact the propagation of travelling waves. Some external stimuli, such as habitat fragmentation, can be severe enough to cause propagation failure.

The study of spreading phenomena in such periodically fragmented landscapes began with the work by Shigesada and co-authors [18]. Their work, which assumed

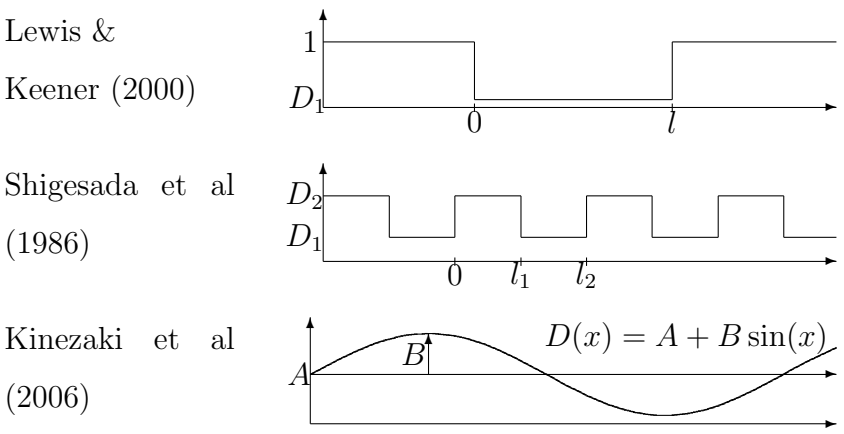

Figure 1.1: Visual representations of the diffusion coefficient $D(x)$ as considered by Lewis & Keener, Shigesada et al ([18] Fig. 1. pp. 145) . and Kinezaki et al. ([8] Fig. 1. pp. 264).

the absence of an Allee effect, has since been generalized substantially [8, 9, 18]. Recently, Maciel and Lutscher considered an RDE in a periodic habitat with an Allee effect [13]. In chapter 2, inspired by the work of Maciel and Lutscher, we adopt a homogenization approach in order to derive an approximation to the speed of invasion.

Following a classical homogenization approach, we successfully derive an expression that provides insight into the relationship between spatial perturbations and successful propagation. However, we observe that this procedure does not provide a complete picture.

In chapter 3, we alter our approach and consider the effects of symmetry-breaking perturbations. Roy and LeBlanc considered the problem of blocking as a two parameter problem [11, 16]. In their paper, they showed that for the semi-linear equation

$$\frac{du}{dt} = \mathcal{A}u + \mathcal{F}(u, c) + \varepsilon\mathcal{G}(u, x; \varepsilon)$$

propagation failure lies inside a cone in the (c, ε) parameter space that emanates out from the origin (see Figure 1.2). In chapter 3, we utilize the ideas of Roy and LeBlanc

and extend their results to include reaction-diffusion equations of the form

$$\frac{\partial u}{\partial t} = \frac{\partial^2 u}{\partial x^2} + \mathcal{F}(u, c) + \varepsilon \mathcal{G}(u_x, u, x; \varepsilon). \tag{1.4.1}$$

In doing so, we show that wave-blocking for equations of the form (1.4.1) also occurs in a cone in the (c, ε) parameter space emanating from the origin. In order to illustrate our result, we compare it with multiple numerical simulations in chapter 4.

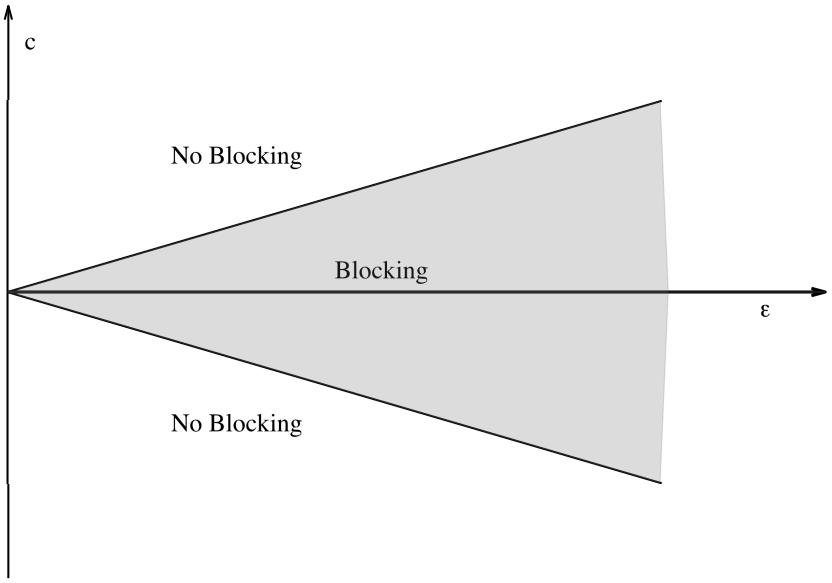

Figure 1.2: The cone of parameter values in (c, ε) parameter space that leads to propagation failure [11, 16].

Chapter 2

Ecological Phenomena

2.1 Ecological Framework

The increased flow of goods and people across the planet has, in turn, increased the rate at which alien species are being introduced to new habitats. Competition between native and alien species can lead to a loss of biodiversity. Hence, it is important to understand the mechanisms that prevent or facilitate the invasion of an alien species.

There is a rich body of literature that suggests many species have reduced reproductive success at low densities [7, 12, 13, 19]. When there exists a positive relationship between the overall individual fitness and population density then the population is said to be subject to a demographic Allee effect [1]. A strong Allee effect is a particular demographic Allee effect in which a population must overcome a particular threshold, called the Allee threshold. There are several mechanisms that may induce an Allee effect, for example pollination failure, reduced mate finding, predation, etc. [1, 13].

A strong Allee effect can be added to the model (1.1.1) by taking the reaction function to be

$$\mathcal{F}(u) = \rho u(1-u)(u-\alpha), \tag{2.1.1}$$

where u is the population density, ρ is the intrinsic growth rate and $\alpha \in [0, 1]$ is the corresponding Allee threshold. Equation (2.1.1) is analogous to the reaction term in (1.1.5). Thus, in a homogeneous, continuous environment the solution of (1.1.1) with (2.1.1) and a monotonic or localized initial distribution will approach a propagating wave with constant speed [18]. Whether the wave speed is positive (successful invasion) or negative (retreating) is determined by the Allee threshold. In the case of (2.1.1) the wave speed is given by [7, 12]

$$c^* = \sqrt{2\rho D}\left(\frac{1}{2} - \alpha\right). \tag{2.1.2}$$

The species is able to successfully invade if $\alpha < 1/2$ and retreats if $\alpha > 1/2$. When $\alpha = \frac{1}{2}$ the invasion front stalls, neither retreating nor advancing. This means that a species introduced at a certain site will remain confined to that site, i.e., the invasion has been pinned. This computation indicates that pinning only occurs for one specific parameter value, which suggests that we would not expect to observe this phenomenon in nature.

2.2 Homogenization

In order to gain a better understanding of how habitat heterogeneity impacts spreading speeds we apply a homogenization procedure. Previous work in this direction indicates that the results from applying homogenization techniques provide an accurate approximation to the exact speed of spread [13, 18]. Here we consider the invasion of a single species into spatially varying environments in one dimension. The movement and population dynamics are governed by the reaction-diffusion equation

$$\frac{\partial u}{\partial t} = \frac{\partial}{\partial x}\left(D(x)\frac{\partial u}{\partial x}\right) + \mathcal{F}(u, x). \tag{2.2.1}$$

The functions $D(x)$ and $\mathcal{F}(u, x)$ denote the spatially varying diffusion coefficient and reaction term, respectively, with $D(x) > 0$.

Hypothesis 2.2.1. We assume that $\mathcal{F}$ and D are periodic in x with period $l > 0$. Then there exist 1-periodic functions $\tilde{D}$ and $\tilde{\mathcal{F}}$ such that $D(x) = \tilde{D}(x/l)$ and $\mathcal{F}(u, x) = \tilde{\mathcal{F}}(u, x/l)$.

It becomes clear from hypothesis 2.2.1 that if $l \ll 1$ then D and $\mathcal{F}$ are rapidly varying functions. Processes modelled by (2.2.1) that satisfy hypothesis 2.2.1 can be quite difficult to study. Thus, it seems reasonable to try and replace equation (2.2.1) with another problem that is independent of the parameter l while still being "close" enough to the original problem. This new problem is the so called homogenized problem.

As a consequence of hypothesis 2.2.1 we can see that the diffusion and reaction terms depend on the variable $y = x/l$. For $l \ll 1$, we write the solution u with the additional small scale variable y. That is $u = u(t, x, y)$ which is 1-periodic in the last argument. With the addition of this small scale variable, we now search for a solution in the form of an asymptotic expansion, that is

$$u(t, x, y) = u_0(t, x, y) + lu_1(t, x, y) + l^2 u_2(t, x, y) + H.O.T.$$

where u_i are periodic in y with period 1 for $i \geq 0$ and u_i have zero mean for $i \geq 1$ [15]. Applying the chain rule the differentiation operator becomes

$$\frac{\partial}{\partial x} \longrightarrow \frac{\partial}{\partial x} + \frac{1}{l}\frac{\partial}{\partial y}.$$

Substituting the asymptotic expansion into (2.2.1) gives us

$$\begin{aligned}\frac{\partial}{\partial t}(u_0 + lu_1 + ...) = \left[\frac{\partial}{\partial x} + \frac{1}{l}\frac{\partial}{\partial y}\right]\left(\tilde{D}(y)\left[\frac{\partial}{\partial x} + \frac{1}{l}\frac{\partial}{\partial y}\right](u_0 + lu_1 + ...)\right) \\ + \tilde{\mathcal{F}}(u_0 + lu_1 + ..., y).\end{aligned}$$

Our goal now is to compare the coefficients of the powers of l and study the resulting equations.

2.2.1 The $O(l^{-2})$ Equation

Substituting the asymptotic expansion into (2.2.1) and collecting powers of l we arrive at the $O(l^{-2})$ equation given by

$$\tilde{D}'(y)\frac{\partial u_0}{\partial y} + \tilde{D}(y)\frac{\partial^2 u_0}{\partial y^2} = 0.$$

This equation can easily be rewritten in the form

$$\frac{\partial}{\partial y}\left[\tilde{D}(y)\frac{\partial u_0}{\partial y}\right] = 0. \tag{2.2.2}$$

Using the periodicity of u_0 along with equation (2.2.2) and the periodicity of $\tilde{D}$ we find that u_0 is independent of y [15].

2.2.2 The $O(l^{-1})$ Equation

Following the same procedure as before, we are able to derive the $O(l^{-1})$ equation

$$\frac{\partial}{\partial y}\left[\tilde{D}(y)\frac{\partial u_1}{\partial y}\right] + \tilde{D}'(y)\frac{\partial u_0}{\partial x} = 0. \tag{2.2.3}$$

Using the fact that u_0 is independent of y and integrating with respect to y, we get

$$\tilde{D}(y)\frac{\partial u_1}{\partial y} + \tilde{D}(y)\frac{\partial u_0}{\partial x} = K_1(t,x)$$

where K_1 is an arbitrary function of t and x. Solving for u_1 we get

$$u_1(t,x,y) = \left[\int_0^y \frac{1}{\tilde{D}(s)}ds\right]K_1(t,x) - y\frac{\partial u_0}{\partial x} + K_2(t,x).$$

where K_2 is also an arbitrary function of t and x [15]. Using the fact that u_1 is periodic in y with period 1, we find that

$$K_1(t,x) = \left[\int_0^1 \frac{1}{\tilde{D}(s)}ds\right]^{-1}\frac{\partial u_0}{\partial x}.$$

Furthermore, imposing the condition that u_1 have zero mean, we find that

$$K_2(t,x) = \left[\frac{1}{2} - \left[\int_0^1 \frac{1}{\tilde{D}(s)}ds\right]^{-1}\left[\int_0^1\int_0^y \frac{1}{\tilde{D}(s)}dsdy\right]\right]\frac{\partial u_0}{\partial x}.$$

Thus $u_1 = H(y)\frac{\partial u_0}{\partial x}$ where

$$H(y) = \frac{1}{2} - y + \left[\int_0^y \frac{1}{\tilde{D}(s)}ds\right]\left[\int_0^1 \frac{1}{\tilde{D}(s)}ds\right]^{-1} - \left[\int_0^1 \frac{1}{\tilde{D}(s)}ds\right]^{-1}\left[\int_0^1\int_0^y \frac{1}{\tilde{D}(s)}dsdy\right].$$

2.2.3 The $O(l^0)$ Equation

As we have done for the previous equations, we compare the coefficients of l^0 and set them equal to each other. Doing so gives the equation

$$\frac{\partial u_0}{\partial t} = \tilde{D}(y)\frac{\partial^2 u_0}{\partial x^2} + \tilde{D}'(y)\frac{\partial u_1}{\partial x} + 2\tilde{D}(y)\frac{\partial^2 u_1}{\partial x \partial y} + \frac{\partial}{\partial y}\left[\tilde{D}(y)\frac{\partial u_2}{\partial y}\right] + \tilde{\mathcal{F}}(u_0, y). \quad (2.2.4)$$

Using the fact that $u_1 = H(y)\frac{\partial u_0}{\partial x}$ we can rewrite (2.2.4) to get

$$\frac{\partial u_0}{\partial t} = (\tilde{D} + \tilde{D}'H + 2\tilde{D}H')\frac{\partial^2 u_0}{\partial x^2} + \frac{\partial}{\partial y}\left[\tilde{D}(y)\frac{\partial u_2}{\partial y}\right] + \tilde{\mathcal{F}}(u_0, y). \quad (2.2.5)$$

Lemma 2.2.2. *$H(y)$ is such that*

$$\int_0^1 (\tilde{D} + \tilde{D}'H + 2\tilde{D}H')dy = \left[\int_0^1 \frac{1}{\tilde{D}(s)}ds\right]^{-1}$$

Proof: For the sake of convenience we will define the constants Γ_1 and Γ_2 such that

$$\Gamma_1 = \left[\int_0^1 \frac{1}{\tilde{D}(s)}ds\right]^{-1}, \qquad \Gamma_2 = \left[\int_0^1 \frac{1}{\tilde{D}(s)}ds\right]^{-1}\left[\int_0^1\int_0^y \frac{1}{\tilde{D}(s)}dsdy\right].$$

Then

$$\tilde{D} + \tilde{D}'H + 2\tilde{D}H' = \frac{\tilde{D}'}{2} - y\tilde{D}' + \Gamma_1\tilde{D}'\left[\int_0^y \frac{1}{\tilde{D}(s)}ds\right] - \Gamma_2\tilde{D}' - \tilde{D} + 2\Gamma_1.$$

Since $\tilde{D}$ is assumed to be periodic in y with period 1 integrating over one period in y gives

$$\int_0^1 (\tilde{D} + \tilde{D}'H + 2\tilde{D}H')dy = 2\Gamma_1 + \Gamma_1\int_0^1 \tilde{D}'\left[\int_0^y \frac{1}{\tilde{D}(s)}ds\right]dy - \int_0^1 y\tilde{D}' + \tilde{D}dy$$

$$= 2\Gamma_1 + \Gamma_1 \int_0^1 \tilde{D}' \left[\int_0^y \frac{1}{\tilde{D}(s)} ds \right] dy - \int_0^1 \frac{d}{dy}(y\tilde{D}) dy$$
$$= 2\Gamma_1 - \tilde{D}(1) + \Gamma_1 \int_0^1 \tilde{D}' \left[\int_0^y \frac{1}{\tilde{D}(s)} ds \right] dy.$$

Integrating by parts we find

$$\int_0^1 \tilde{D}' \left[\int_0^y \frac{1}{\tilde{D}(s)} ds \right] dy = \tilde{D}(y) \left[\int_0^y \frac{1}{\tilde{D}(s)} ds \right] \Big|_0^1 - \int_0^1 \tilde{D}(y) \frac{1}{\tilde{D}(y)} dy$$
$$= \frac{\tilde{D}'(1)}{\Gamma_1} - 1.$$

Thus, integrating over one period of y gives

$$\int_0^1 (\tilde{D} + \tilde{D}'H + 2\tilde{D}H')dy = 2\Gamma_1 - \tilde{D}(1) + \Gamma_1 \left(\frac{\tilde{D}'(1)}{\Gamma_1} - 1 \right) = \Gamma_1.$$

as desired. □

Now we integrate equation (2.2.5) over one period in y. Using the periodicity of $\tilde{D}$ and u_2 as well as lemma 2.2.2 we find that the leading order term u_0 satisfies

$$\frac{\partial u_0}{\partial t} = \langle \tilde{D} \rangle_H \frac{\partial^2 u_0}{\partial x^2} + \langle \tilde{\mathcal{F}} \rangle_A. \tag{2.2.6}$$

Here $\langle \cdot \rangle_H$ and $\langle \cdot \rangle_A$ denote the harmonic and arithmetic means respectively. That is

$$\langle \tilde{D} \rangle_H = \left[\int_0^1 \frac{1}{\tilde{D}(y)} dy \right]^{-1}, \qquad \langle \tilde{\mathcal{F}} \rangle_A = \int_0^1 \tilde{\mathcal{F}}(u_0, y) dy.$$

2.3 Homogenization and Invasion Pinning

We consider the same situation as [13, 19]; the species experiences a strong Allee effect that varies in space. Accordingly, we choose the growth function in (2.2.1) to be

$$\mathcal{F}(u, x) = \rho(x)u(1 - u)(u - \alpha(x)) \tag{2.3.1}$$

where $\rho(x)$ and $\alpha(x)$ denote the spatially varying intrinsic growth rate and Allee threshold respectively. If we proceed by homogenization as outlined in the previous

section then our goal is to write the homogenized growth function in the standard cubic form. If hypothesis 2.2.1 is satisfied then equation (2.2.6) takes the form

$$\frac{\partial u_0}{\partial t} = \langle \tilde{D} \rangle_H \frac{\partial^2 u_0}{\partial x^2} + \int_0^1 \tilde{\rho}(y) u_0 (1 - u_0)(u_0 - \tilde{\alpha}(y)) dy. \tag{2.3.2}$$

where $\rho(x) = \tilde{\rho}(x/l)$ and $\alpha(x) = \tilde{\alpha}(x/l)$. Our goal now is to use the fact that u_0 is independent of y to rewrite the growth function in the standard cubic form.

$$\begin{aligned}
\int_0^1 \tilde{\rho}(y) u_0 (1 - u_0)(u_0 - \tilde{\alpha}(y)) dy &= u_0 \int_0^1 \tilde{\rho}(y)(u_0 - u_0^2 + \tilde{\alpha}(y) u_0 - \tilde{\alpha}(y)) dy \\
&= u_0 \left(\left[\int_0^1 \tilde{\rho}(y) dy \right] u_0 - \left[\int_0^1 \tilde{\rho}(y) dy \right] u_0^2 \right. \\
&\quad \left. + \left[\int_0^1 \tilde{\rho}(y) \tilde{\alpha}(y) dy \right] u_0 - \left[\int_0^1 \tilde{\rho}(y) \tilde{\alpha}(y) dy \right] \right).
\end{aligned}$$

Letting $P_1 = \int_0^1 \tilde{\rho}(y) dy$ and $P_2 = \int_0^1 \tilde{\rho}(y) \tilde{\alpha}(y) dy$ we are able to write out a simplified version of the reaction term that we can factor.

$$\begin{aligned}
\int_0^1 \tilde{\rho}(y) u_0 (1 - u_0)(u_0 - \tilde{\alpha}(y)) dy &= P_1 u_0 \left(-u_0^2 + \left(1 + \frac{P_2}{P_1} \right) u_0 - \frac{P_2}{P_1} \right) \\
&= P_1 u_0 (1 - u_0) \left(u_0 - \frac{P_2}{P_1} \right)
\end{aligned}$$

Thus, the homogeneous equation (2.3.2) can be rewritten in the form

$$\frac{\partial u_0}{\partial t} = \langle D \rangle_H \frac{\partial^2 u_0}{\partial x^2} + P_1 u_0 (1 - u_0) \left(u_0 - \frac{P_2}{P_1} \right) \tag{2.3.3}$$

which is analogous to the homogenized equation derived by Maciel and Lutscher [13]. In the presence of a strong Allee effect they showed, numerically, that in the limit $l \to 0$ the spreading speed of the heterogeneous equation is approximately that of the homogeneous equation [13]. Solutions to (2.3.3) with monotonic or localized initial distributions converge to a travelling wave front with a constant velocity given by [7]

$$c_{approx} = \sqrt{2 \langle D \rangle_H P_1} \left(\frac{1}{2} - \frac{P_2}{P_1} \right). \tag{2.3.4}$$

From this expression we expect the invasion to advance if $P_2/P_1 < 1/2$, to retreat if $P_2/P_1 > 1/2$ and to stall when $P_2/P_1 = 1/2$. The latter phenomenon has been termed "invasion pinning" and is particularly interesting when trying to manage an invasive pest species.

Example. Consider the case where $D(x) = A + B\sin(x)$, $\alpha(x) = \alpha$ and $\rho(x) = 1$ where α, A and B are parameters. Since $D(x)$ is periodic with period 2π it follows that $l = 2\pi$ and $\tilde{D}(y) = A + B\sin(2\pi y)$. Thus, applying equation (2.3.4) we get

$$c_{approx} = \sqrt{2\left[\int_0^1 \frac{1}{\tilde{D}(y)}dy\right]^{-1}}\left(\frac{1}{2} - \alpha\right).$$

Figure 2.1 illustrates c_{approx} as a function of B for $A = 1, 2, 3, 4$ and $\alpha = 0.4646$. In particular, Figure 2.1 shows us that invasion pinning only occurs for a small range of parameter values, specifically $A = B$. However, the simulations in Figure 2.2 show that when $A = 1$ and B is small the wave still propagates but invasion pinning occurs for larger values of $B < 1$ with $c_{approx} \neq 0$.

These results are not entirely surprising. Maciel and Lutscher noticed that when l is not small, the approximation can be very poor and invasion pinning can occur for a relatively large range of parameter values [13]. Also, Musgrave and co-authors [14] studied invasion pinning in a discrete-time model and gave some estimates for when pinning occurs when l is not small. As they pointed out, it is clear that standard homogenization techniques alone cannot work for large spatial periods. Keener proposed an alternative homogenization approach to study invasion pinning, but his technique depends on appropriate changes of variables and is highly case specific [4].

In the next chapter, we will present an alternative approach to studying invasion pinning. This will be done by focusing on the relationship between the speed of the travelling wave and the strength of the perturbation. The results presented in the next section are derived by exploiting the translational symmetry of the underlying system.

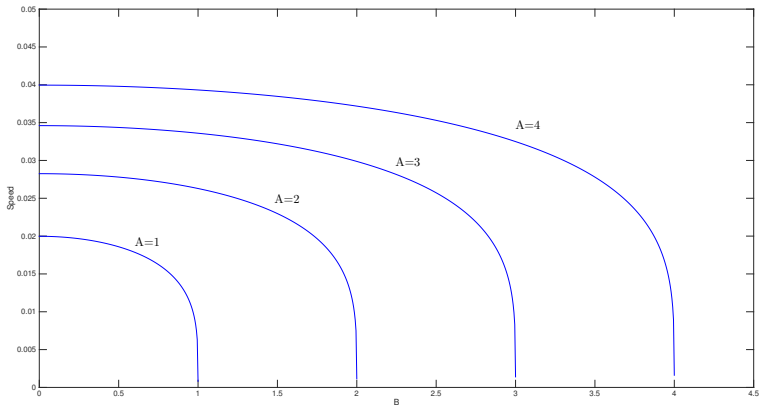

Figure 2.1: Plot of the homogenized speed c_{approx} as a function of the parameter B for fixed values of $A = 1, 2, 3, 4$ and $\alpha = 0.4646$.

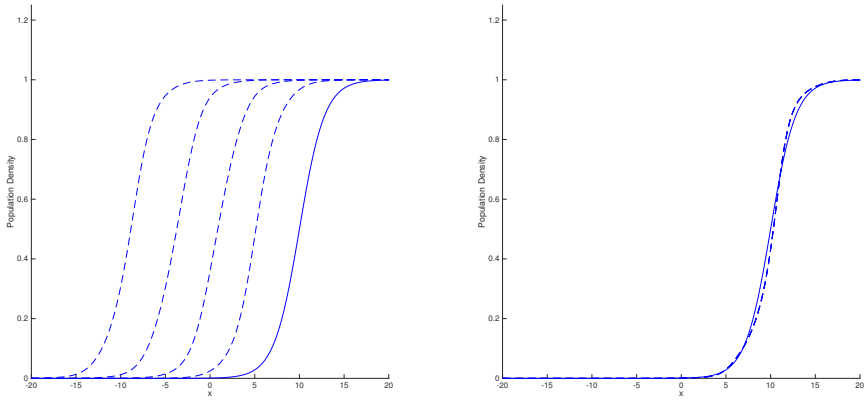

Figure 2.2: Evolution of a travelling wave solution of equation (2.2.1) with (2.3.1), $D(x) = 1 + B\sin(x)$, $\alpha(x) = \alpha$ and $\rho(x) = 1$. The initial wave profile is given by a solid line while the successive snapshots taken at regular time intervals, are given by the dashed lines. Parameters are $\alpha = 0.4646$, and $B = 0.1$ (left), $B = 0.35$ (right)

Chapter 3

Wave Blocking Phenomena

In this chapter, we study wave blocking phenomena by adopting a symmetry-breaking perturbation approach developed by LeBlanc and Roy [11, 16]. The theory presented here is built upon two key observations. The first is that a large class of PDEs on $\mathbb{R}^n$, for any n, can be expressed in the form of a dynamical system [3, 10] and the second is that many of these equations share a common characteristic: they admit a symmetry group [10].

When we think of symmetry in n-dimensional euclidean space we immediately think of translational and rotational symmetry. Together translations and rotations generate the special Euclidean group $SE(n)$. The group $\Gamma = SE(n)$ can act as a symmetry on some space X. In particular, a group Γ acts on a space X if there is a map

$$\Gamma \times X \to X; (g, x) \to g \cdot x$$

such that

1. $e \cdot x = x$ where $e \in \Gamma$ is the identity of Γ;
2. $g \cdot (h \cdot x) = (gh) \cdot x$ for $g, h \in \Gamma$.

Our interest lies in group equivariant mappings. Suppose that Γ is a group acting on a vector space X. Then the function $\mathcal{F} : X \to Y$ is Γ-equivariant if $\mathcal{F}(g \cdot u) = g \cdot \mathcal{F}(u)$ for every $g \in \Gamma$, $u \in X$. It is well known that equation (1.1.1) is equivariant with respect to the group action of the special euclidean group $SE(n)$ [17]. Thus $SE(n)$ is a symmetry group of (1.1.1).

3.1 Setup

In order to understand the relationship between spatial heterogeneities and propagation failure, we formulate (1.1.1) as dynamical system on an appropriate Banach space. That is

$$\frac{du}{dt} = \mathcal{A}u + \mathcal{F}(u, \alpha) + \varepsilon \mathcal{G}(\xi u, u, x; \varepsilon), \tag{3.1.1}$$

where $\xi = \frac{\partial}{\partial x}$, $\mathcal{A} = \frac{\partial^2}{\partial x^2}$ denotes the diffusion operator, α and ε are real parameters, ε small, and $\mathcal{G}$ is a function representing the spatial inhomogeneity. Furthermore, we make the following assumptions about the reaction term $\mathcal{F}(u, \alpha)$.

Hypothesis 3.1.1. Function $\mathcal{F}$ is smooth with $\mathcal{F}(0, \alpha) = \mathcal{F}(\alpha, \alpha) = \mathcal{F}(1, \alpha) = 0$. Furthermore, $\mathcal{F}(u, \alpha) < 0$ for $u \in (0, \alpha)$ and $\mathcal{F}(u, \alpha) > 0$ for $u \in (\alpha, 1)$.

As a specific example we take $\mathcal{F}(u, \alpha)$ to be the same as (1.3.4). One of the advantages for doing this is that we can derive an explicit travelling wave solution for the unperturbed system ($\varepsilon = 0$). In particular the profile of this wave is given by [6, 16]

$$u^*(x) = \frac{1}{2}\left(1 + \tanh\left(\frac{x}{2\sqrt{2}}\right)\right). \tag{3.1.2}$$

We note that, for this particular choice of $\mathcal{F}$, the wave profile is independent of the parameter α. However, all the ideas presented here can be applied to systems much more general than the system where $\mathcal{F}$ is given by (1.3.4). We chose to restrict our analysis to this particular case for computational ease.

It is also a well known fact that reaction diffusion equations of the form

$$\frac{du}{dt} = \mathcal{A}u + \mathcal{F}(u, \alpha) \tag{3.1.3}$$

are well posed on the spaces $C^0_{unif}(\mathbb{R}, \mathbb{R})$ and $L^2(\mathbb{R}, \mathbb{R})$ [17]. Furthermore, equation (3.1.3) generates a local semiflow on both $C^0_{unif}(\mathbb{R}, \mathbb{R})$ and $L^2(\mathbb{R}, \mathbb{R})$ [11, 16, 17]. However, travelling fronts exist in $C^0_{unif}(\mathbb{R}, \mathbb{R})$ and not in $L^2(\mathbb{R}, \mathbb{R})$. Thus, we work in the Banach space of bounded uniformly continuous functions $Y = C^0_{unif}(\mathbb{R}, \mathbb{R})$.

In order to help us visualize the symmetry of our problem, we consider the special euclidean group $\Gamma = SE(1)$ which we take to be the group of rigid translations on the real line. Now let $\mathcal{T} : \Gamma \to GL(Y)$ be an isometric representation of Γ. Thus, for any $a \in \Gamma$ and for any $f \in Y$ we have $\mathcal{T}_a f(x) = f(x + a)$ where $\mathcal{T}_a$ denotes $\mathcal{T}(a)$.

The infinitesimal generator of the translation $\mathcal{T} : a \mapsto \mathcal{T}_a$ is given by the derivative

$$\xi u = \lim_{h \to 0} \frac{\mathcal{T}_h u(x) - u(x)}{h} = \frac{\partial u}{\partial x}. \tag{3.1.4}$$

Operators $\mathcal{A}$ and ξ are defined on dense subspaces of Y, and we observe that they commute with $\mathcal{T}_a$ and with each other, i.e $\mathcal{A}\xi = \xi\mathcal{A}$, $\mathcal{A}\mathcal{T}_a = \mathcal{T}_a\mathcal{A}$ and $\xi\mathcal{T}_a = \mathcal{T}_a\xi$ on appropriate dense spaces of Y.

Hypothesis 3.1.2. We make the following assumptions on the functions $\mathcal{F}$ and $\mathcal{G}$:

(i) $\mathcal{F}$ is Γ-equivariant, that is $\mathcal{F}(\mathcal{T}_a u, \alpha) = \mathcal{T}_a \mathcal{F}(u, \alpha)$.

(ii) The bounded function $\mathcal{G}$ is smooth and not Γ-equivariant. That is, there exists $a \in \Gamma$ such that

$$\mathcal{G}(\xi\mathcal{T}_a u, \mathcal{T}_a u, x; \varepsilon) \neq \mathcal{T}_a \mathcal{G}(\xi u, u, x; \varepsilon). \tag{3.1.5}$$

Since our goal is to study the relationship between spatial perturbations and the speed of propagation, we suspend c, the wave speed parameter, and consider the system

$$\begin{aligned} u_t &= \mathcal{A}u + \mathcal{F}(u, \alpha(c)) + \varepsilon\mathcal{G}(\xi u, u, x; \varepsilon), \\ c_t &= 0. \end{aligned} \tag{3.1.6}$$

Accordingly we study this system on the space $Y \times \mathbb{R}$. We extend the group action of $\mathcal{T}$ such that

$$\mathcal{T}_a \begin{pmatrix} u(x) \\ c \end{pmatrix} = \begin{pmatrix} \mathcal{T}_a u(x) \\ c \end{pmatrix},$$

and we define the scalar product on $Y \times \mathbb{R}$ to be

$$\left\langle \begin{pmatrix} u(x) \\ a \end{pmatrix}, \begin{pmatrix} v(x) \\ b \end{pmatrix} \right\rangle = \int_{-\infty}^{\infty} u(x)v(x)dx + ab \tag{3.1.7}$$

for functions u and v such that the integral converges. We also define the norm on $Y \times \mathbb{R}$ to be

$$\begin{aligned} \left\| \begin{pmatrix} u(x) \\ a \end{pmatrix} \right\| &= \|u(x)\| + |a| \\ &= \sup_{x \in \mathbb{R}} |u(x)| + |a|. \end{aligned}$$

3.2 Relative Equilibria and Wave Speed

We begin our analysis by letting $\varepsilon = 0$ in (3.1.6) and focusing on the unperturbed system

$$\begin{aligned} u_t &= Au + \mathcal{F}(u, \alpha), \\ c_t &= 0. \end{aligned} \tag{3.2.1}$$

As a consequence of hypothesis 3.1.2, equation (3.1.3) is equivariant with respect to the action of Γ. In the special case of the traveling wave solution, u^*, the time-orbit of the RDE is contained in the Γ-orbit of the group action. Such a solution is called a *relative equilibrium* [17].

For the system (3.2.1) the relative equilibrium is a solution of the form

$$\begin{pmatrix} u(t) \\ c(t) \end{pmatrix} = \begin{pmatrix} \mathcal{T}_{a(t)} u^* \\ c \end{pmatrix}, \tag{3.2.2}$$

with $a(t) = ct$ for (3.2.1). Substituting this parameterization of the relative equilibrium and applying hypothesis 3.1.2 we get

$$\mathcal{T}_{ct} c\xi u^* = \mathcal{T}_{ct}\mathcal{A}u^* + \mathcal{T}_{ct}\mathcal{F}(u^*, \alpha).$$

Since Γ is a group, every element is invertible and so we can cancel out the translations.

Hypothesis 3.2.1. We assume that there is an interval $I \subset \mathbb{R}$ for the parameter α, such that the traveling wave speed $c = c(\alpha)$ is a smooth function defined by

$$c(\alpha)\xi u^* = \mathcal{A}u^* + \mathcal{F}(u^*, \alpha). \tag{3.2.3}$$

Furthermore, we assume that there exists $\alpha_0 \in I$ such that $c(\alpha_0) = 0$ and $c'(\alpha_0) \neq 0$.

By choosing $\mathcal{F}(u, \alpha) = u(1-u)(u-\alpha)$ we know that c and α are related via the formula $c(\alpha) = \frac{1-2\alpha}{\sqrt{2}}$. By virtue of this hypothesis we can invert the relation between c and α and use c as a parameter, writing $\mathcal{F}(u, c)$ instead. As a result equation (3.2.3) can be rewritten as

$$c\xi u^* = \mathcal{A}u^* + \mathcal{F}(u^*, c). \tag{3.2.4}$$

3.3 The Linear Operator L

When $c = 0$, applying ξ to (3.2.4) and using the commutativity of $\mathcal{A}$ and ξ we get the identity

$$\mathcal{A}(\xi u^*) + \mathcal{F}_u(u^*, 0)\xi u^* = 0.$$

Similarly, differentiating (3.2.4) with respect to c and evaluating at $c = 0$ gives

$$\mathcal{A}u_c^* + \mathcal{F}_u(u^*, 0)u_c^* + \mathcal{F}_c(u^*, 0) = \xi u^*. \tag{3.3.1}$$

In the case where our wave profile is independent of α and hence independent of c, the above equality reduces to $\mathcal{F}_c(u^*, 0) = \xi u^*$. Inspired by these identities, we consider

the densely defined operator $L : Y \times \mathbb{R} \to Y \times \mathbb{R}$

$$L \begin{pmatrix} \phi \\ w \end{pmatrix} = \begin{pmatrix} \mathcal{A}\phi + \mathcal{F}_u(u^*, 0)\phi + \mathcal{F}_c(u^*, 0)w \\ 0 \end{pmatrix}. \tag{3.3.2}$$

Hypothesis 3.3.1. (*Spectral Gap Condition ([11], Hypothesis 3.3a, p 13)*) Assume that the zero eigenvalue of L is such that the corresponding generalized eigenspace is finite dimensional. Furthermore, we will assume that all other elements of the spectrum of L are bounded away from the imaginary axis.

We observe that

$$L \begin{pmatrix} \xi u^* \\ 0 \end{pmatrix} = \begin{pmatrix} 0 \\ 0 \end{pmatrix} \quad \text{and} \quad L \begin{pmatrix} 0 \\ 1 \end{pmatrix} = \begin{pmatrix} \xi u^* \\ 0 \end{pmatrix}, \tag{3.3.3}$$

i.e, L has a zero eigenvalue with (generalized) eigenvectors given by $\psi_1 = (\xi u^*, 0)^T$ and $\psi_2 = (0, 1)^T$. It was shown in [11, 16] that the generalized eigenspace associated with the 0 eigenvalue is $E = \text{span}\{\psi_1, \psi_2\}$. Thus the corresponding generalized eigenspace is finite dimensional as required.

It remains to be shown that all other elements of the spectrum of L are bounded away from the imaginary axis. We define the spectrum of L to be the set of complex numbers λ such that the operator $(L - \lambda I)$ is not invertible. In order to study the spectrum of L, denoted by $\sigma(L)$, we must enlist the aide of the operators

$$\mathcal{L}_1\phi = \phi'' + G(x)\phi \tag{3.3.4}$$

$$\mathcal{L}_2 \begin{pmatrix} \phi \\ w \end{pmatrix} = \begin{pmatrix} \mathcal{L}_1\phi + \mathcal{F}_c(u^*, 0)w \\ 0 \end{pmatrix}. \tag{3.3.5}$$

Suppose that $G(x) \to G_\pm$ as $x \to \pm\infty$ and assume without loss of generality that $G_- < G_+$. Then it is shown in [3] that

$$\max\{\text{Re}(\sigma(\mathcal{L}_1))\} = \max\{G_-, G_+\} = G_+.$$

Thus if $G_+ < 0$ then the spectrum of $\mathcal{L}_1$ is bounded away from the imaginary axis in the left half plane. Furthermore, it was shown in [16] that when $\mathcal{F}_c(u^*, 0) = \xi u^*$ then $\sigma(\mathcal{L}_2) \subseteq \sigma(\mathcal{L}_1)$. For the operator $\mathcal{L}_1$ with $G(x) = \mathcal{F}_u(u^*, 0)$ then $L = \mathcal{L}_2$ and so applying these results tells us that the spectrum of L is also bounded away from the imaginary axis, in the left half plane, with the exception of the zero eigenvalue.

Hypothesis 3.3.1 ensures the stability of our relative equilibrium and in turn guarantees that solutions will persist after being lightly perturbed. It follows from LeBlanc and Roy [11, 16] that the projection operator

$$P\begin{pmatrix} v(x) \\ c \end{pmatrix} = \frac{\left\langle \psi_1, \begin{pmatrix} v(x) \\ c \end{pmatrix} \right\rangle}{\langle \psi_1, \psi_1 \rangle} \psi_1 + \frac{\left\langle \psi_2, \begin{pmatrix} v(x) \\ c \end{pmatrix} \right\rangle}{\langle \psi_2, \psi_2, \rangle} \psi_2 \tag{3.3.6}$$

defines an L-invariant splitting of the space $Y \times \mathbb{R} = \text{range}(P) \oplus \ker(P) = E \oplus W$ with the scalar product as defined by (3.1.7).

3.4 The Centre Manifold

Hypothesis 3.4.1. We will assume that

(i) The map $a \to \mathcal{T}_a u^*$ is C^{k+2}.

(ii) The map $a \to \mathcal{T}_a v$ is C^{k+2} whenever $v \in E$.

(iii) For all $K > 0$, $\exists \delta > 0$ such that $\|\mathcal{T}_a u^* - u\| \geq \delta$ whenever $|a| > K$.

(iv) The projections $\mathcal{T}_a P \mathcal{T}_{-a}$ are C^{k+1} in $a \in \Gamma$ in the operator norm.

For the scalar bistable reaction-diffusion equation, hypothesis 3.4.1 was verified in [11, 16]. Combining this with the fact that the spectral condition of LeBlanc and Roy is verified we can apply the following centre manifold theorem of Sandstede et al. [17].

Theorem 3.4.2. *([17], Theorem 1, p. 127) Assume that Hypotheses 3.4.1 and the spectral gap condition are obeyed. Under these conditions, there exists a Γ-invariant manifold $\mathcal{S}$ which is locally invariant under the flow Φ_t for any $t \geq 0$. The manifold $\mathcal{S}$ and the action of Γ on $\mathcal{S}$ are of class C^{k+1}. Furthermore, $\mathcal{S}$ is locally exponentially attracting and contains all solutions that stay close to the group orbit of u^* for all backward times.*

Applying theorem 3.4.2 we find that the set

$$\mathcal{S} = \left\{ \begin{pmatrix} \mathcal{T}_a u^* \\ c \end{pmatrix} ; a \in \Gamma, c \in \mathbb{R} \right\}$$

describes the smooth invariant centre manifold for (3.2.1) (see figure 3.1). In particular, the line of equilibria given by $c = 0$ of (3.4.5) corresponds to the group orbit

$$\Theta = \left\{ \begin{pmatrix} \mathcal{T}_a u^* \\ 0 \end{pmatrix} ; a \in \Gamma \right\}$$

of the steady state $(u^*, 0)^T$ of (3.2.1).

Our goal now is describe the dynamics of (3.2.1) restricted to $\mathcal{S}$. The authors in [11, 16, 17] showed that

$$\begin{pmatrix} u \\ c \end{pmatrix} = \mathcal{T}_a \left[\begin{pmatrix} u^* \\ 0 \end{pmatrix} + c \begin{pmatrix} 0 \\ 1 \end{pmatrix} + \begin{pmatrix} \zeta \\ 0 \end{pmatrix} \right] \tag{3.4.1}$$

gives us a representation of the centre manifold. Here ζ accounts for the shape of the wave depending on the speed c. In the case where the wave profile is independent of c we take $\zeta = 0$. Now we substitute (3.4.1) into (3.2.1) to get

$$a_t \mathcal{T}_a \begin{pmatrix} \xi u^* \\ 0 \end{pmatrix} = \mathcal{T}_a \begin{pmatrix} \mathcal{A} u^* \\ 0 \end{pmatrix} + \mathcal{T}_a \begin{pmatrix} \mathcal{F}(u^*, c) \\ 0 \end{pmatrix}.$$

We know that u^* is a steady state solution of (3.2.1) and so

$$\begin{pmatrix} 0 \\ 0 \end{pmatrix} = \begin{pmatrix} \mathcal{A} u^* \\ 0 \end{pmatrix} + \begin{pmatrix} \mathcal{F}(u^*, 0) \\ 0 \end{pmatrix}. \tag{3.4.2}$$

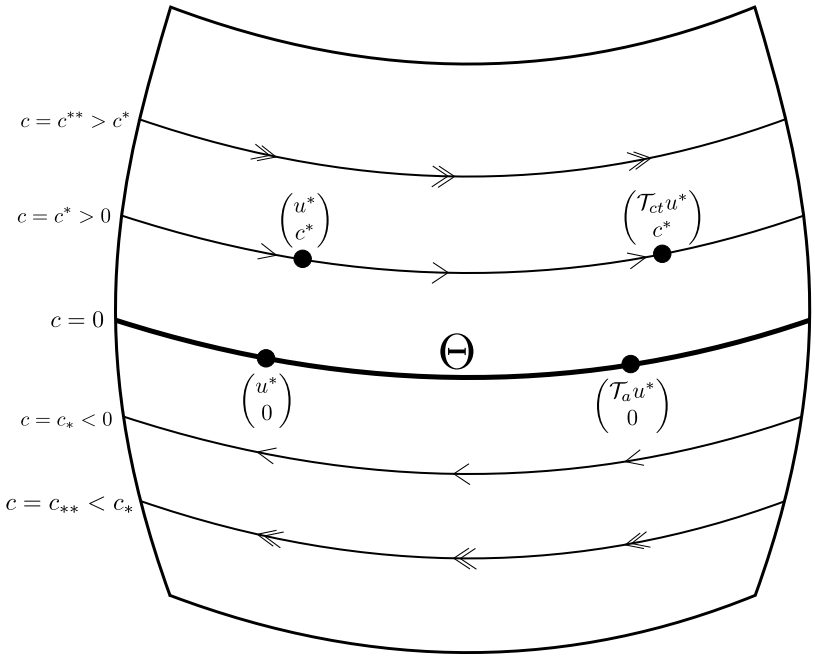

Figure 3.1: The relative equilibria on the unperturbed manifold ([11] Figure 2 p. 25).

Furthermore, applying the definition of L and utilizing equation (3.3.1) with the assumption that the wave profile is independent of c we find that

$$L \begin{pmatrix} 0 \\ c \end{pmatrix} = \begin{pmatrix} c\mathcal{F}_c(u^*, 0) \\ 0 \end{pmatrix} = c \begin{pmatrix} \xi u^* \\ 0 \end{pmatrix}. \tag{3.4.3}$$

Applying $\mathcal{T}_{-a}$ and utilizing both of these identities we get

$$\begin{aligned} a_t \begin{pmatrix} \xi u^* \\ 0 \end{pmatrix} &= L \begin{pmatrix} 0 \\ c \end{pmatrix} + \begin{pmatrix} \mathcal{F}(u^*, c) \\ 0 \end{pmatrix} - \begin{pmatrix} \mathcal{F}(u^*, 0) \\ 0 \end{pmatrix} - \begin{pmatrix} c\mathcal{F}_c(u^*, 0) \\ 0 \end{pmatrix}, \\ &= c \begin{pmatrix} \xi u^* \\ 0 \end{pmatrix} + \begin{pmatrix} H \\ 0 \end{pmatrix} \end{aligned}$$

where $H = \mathcal{F}(u^*, c) - \mathcal{F}(u^*, 0) - \mathcal{F}_c(u^*, 0)c$. We observe that when $\mathcal{F}$ is the same as the cubic nonlinearity in (1.1.5) and u^* is the corresponding wave profile then $H = 0$. Taking this into account we arrive at the compatibility condition

$$\mathcal{F}(u^*, c) - \mathcal{F}(u^*, 0) - \mathcal{F}_c(u^*, 0)c = 0. \tag{3.4.4}$$

Given this information we now observe that the dynamics of (3.2.1) restricted to the centre manifold are governed by the system of equations [11, 16]

$$\begin{aligned} a_t &= c, \\ c_t &= 0. \end{aligned} \tag{3.4.5}$$

We remark that (3.4.4) was derived when u^* is independent of ζ. When $\zeta \neq 0$ then we get the same compatibility condition as LeBlanc and Roy [11, 16]. We also note that these results are not surprising as for the unperturbed problem we anticipated $a(t) = ct$.

3.5 Wave-Blocking in the Perturbed System

Building off the work of LeBlanc and Roy [11, 16] we now prove that wave-blocking for equations of the form 1.4.1 occurs in a wedge in the (c, ε) parameter space emanating from $(0, 0)$. To do this we consider the perturbed system (3.1.6). If ε is small enough then we expect that $\mathcal{S}$ will persist as an invariant manifold in the perturbed system. We denote by $\mathcal{S}_\varepsilon$ the invariant centre manifold for the perturbed system. Even though $\mathcal{S}_\varepsilon$ and $\mathcal{S}$ are diffeomorphic to each other, the dynamics on $\mathcal{S}_\varepsilon$ may differ from those on $\mathcal{S}$.

Let $(u, c)^T$ be a solution of (3.1.6) on $\mathcal{S}_\varepsilon$ close to the group orbit that corresponds to the line of equilibria $c = 0$. We want to use a local decomposition similar to that of (3.4.1) except now we add a term proportional to ε to account for the effects of the perturbation.

$$\begin{pmatrix} u \\ c \end{pmatrix} = \mathcal{T}_a \left[\begin{pmatrix} u^* \\ 0 \end{pmatrix} + c \begin{pmatrix} 0 \\ 1 \end{pmatrix} + \varepsilon \begin{pmatrix} w \\ 0 \end{pmatrix} \right], \tag{3.5.1}$$

It follows that since the perturbation, $\mathcal{G}$, is smooth and bounded then w is a smooth bounded function [11, 16]. Now recall that $\mathcal{G}$ depends on ξu. In order to extend the

results of LeBlanc & Roy to include perturbations of this form we require that w be bounded with respect to ξ.

Proposition 3.5.1. The dynamics on the perturbed centre manifold are governed by the system of equations

$$\begin{aligned} a_t &= c - \varepsilon r(a) + \varepsilon q(a, c, \varepsilon), \\ c_t &= 0, \end{aligned} \tag{3.5.2}$$

where $q(a, c, \varepsilon)$ is a smooth function such that $q \to 0$ uniformly as $(\varepsilon, c) \to (0, 0)$ and

$$r(a) = -\frac{1}{\langle \psi_1, \psi_1 \rangle} \int_{-\infty}^{\infty} \mathcal{T}_{-a} \mathcal{G}(\xi \mathcal{T}_a u^*, \mathcal{T}_a u^*, x, 0) \cdot \xi u^* dx. \tag{3.5.3}$$

Proof: To prove this proposition we substitute parameterization (3.5.1) into system (3.1.6). We find:

$$\begin{aligned} \dot{a}(t)\mathcal{T}_{a(t)} \left(\begin{pmatrix} \xi u^* \\ 0 \end{pmatrix} + O(\varepsilon) \right) &= \mathcal{T}_{a(t)} \left(\begin{pmatrix} \mathcal{A}u^* \\ 0 \end{pmatrix} + \begin{pmatrix} \varepsilon \mathcal{A} w \\ 0 \end{pmatrix} \right) \\ &\quad + \mathcal{T}_{a(t)} \begin{pmatrix} \mathcal{F}(u^* + \varepsilon w, c) \\ 0 \end{pmatrix} \\ &\quad + \varepsilon \begin{pmatrix} \mathcal{G}(\mathcal{T}_a(\xi u^* + \varepsilon \xi w), \mathcal{T}_a(u^* + \varepsilon w), x, \varepsilon) \\ 0 \end{pmatrix}. \end{aligned}$$

Applying $\mathcal{T}_{-a(t)}$ to both sides of the equation above gives

$$\begin{aligned} \dot{a}(t) \left(\begin{pmatrix} \xi u^* \\ 0 \end{pmatrix} + O(\varepsilon) \right) &= \left(\begin{pmatrix} \mathcal{A}u^* \\ 0 \end{pmatrix} + \begin{pmatrix} \varepsilon \mathcal{A} w \\ 0 \end{pmatrix} \right) + \begin{pmatrix} \mathcal{F}(u^* + \varepsilon w, c) \\ 0 \end{pmatrix} \\ &\quad + \varepsilon \begin{pmatrix} \mathcal{T}_{-a(t)} \mathcal{G}(\mathcal{T}_a(\xi u^* + \varepsilon \xi w), \mathcal{T}_a(u^* + \varepsilon w), x, \varepsilon) \\ 0 \end{pmatrix}. \end{aligned}$$

Now we utilize (3.4.2), (3.4.3) as well as the fact that

$$L \begin{pmatrix} \varepsilon w \\ 0 \end{pmatrix} = \begin{pmatrix} \varepsilon A w + \varepsilon \mathcal{F}_u(u^*, 0) w \\ 0 \end{pmatrix},$$

to rewrite the previous expression as

$$\dot{a}(t)\left(\begin{pmatrix}\xi u^*\\0\end{pmatrix}+O(\varepsilon)\right)=L\begin{pmatrix}0\\c\end{pmatrix}+\varepsilon L\begin{pmatrix}w\\0\end{pmatrix}+\begin{pmatrix}\mathcal{F}(u^*+\varepsilon w,c)\\0\end{pmatrix}$$
$$-\begin{pmatrix}\mathcal{F}(u^*,0)\\0\end{pmatrix}-\begin{pmatrix}\mathcal{F}_c(u^*,0)c\\0\end{pmatrix}-\varepsilon\begin{pmatrix}\mathcal{F}_u(u^*,0)w\\0\end{pmatrix}$$
$$+\varepsilon\begin{pmatrix}\mathcal{T}_{-a(t)}\mathcal{G}(\mathcal{T}_{a(t)}(\xi u^*+\varepsilon\xi w),\mathcal{T}_{a(t)}(u^*+\varepsilon w),x,\varepsilon)\\0\end{pmatrix}.$$

Hypothesis 3.1.2, along with the fact that w is a uniformly continuous function and bounded with respect to ξ, tells us that as $(\varepsilon,c)\to(0,0)$ the difference

$$\mathcal{T}_{-a}\mathcal{G}(\mathcal{T}_a(\xi u^*+\varepsilon\xi w),\mathcal{T}_a(u^*+\varepsilon w),x,\varepsilon)-\mathcal{T}_{-a}\mathcal{G}(\mathcal{T}_a(\xi u^*),\mathcal{T}_a u^*,x,0)\tag{3.5.4}$$

tends to zero. Thus we introduce the function

$$q(a,c,\varepsilon)=\frac{1}{\varepsilon}(\mathcal{F}(u^*+\varepsilon w,c)-\mathcal{F}(u^*,c))-\mathcal{F}_u(u^*,c)w+\mathcal{F}_u(u^*,c)w-\mathcal{F}_u(u^*,0)w$$
$$+\mathcal{T}_{-a}\mathcal{G}(\mathcal{T}_a(\xi u^*+\varepsilon\xi w),\mathcal{T}_a(u^*+\varepsilon w),x,\varepsilon)-\mathcal{T}_{-a}\mathcal{G}(\mathcal{T}_a(\xi u^*),\mathcal{T}_a u^*,x,0)$$

where $q(a,c,\varepsilon)\to 0$ as $(\varepsilon,c)\to(0,0)$. Adding and subtracting $(\varepsilon q,0)^T$ from the equation gives us

$$\dot{a}(t)\left(\begin{pmatrix}\xi u^*\\0\end{pmatrix}+O(\varepsilon)\right)=L\begin{pmatrix}0\\c\end{pmatrix}+\varepsilon L\begin{pmatrix}w\\0\end{pmatrix}+\begin{pmatrix}H\\0\end{pmatrix}$$
$$+\varepsilon\begin{pmatrix}\mathcal{T}_{-a}\mathcal{G}(\mathcal{T}_a(\xi u^*),\mathcal{T}_a u^*,x,0)\\0\end{pmatrix}+\varepsilon\begin{pmatrix}q\\0\end{pmatrix}.$$

Applying the projection P to the above equation and using (3.4.4) as well as the fact that $L(0,c)^T=c(\xi u^*,0)^T$ and $P(\xi u^*,0)=(\xi u^*,0)=\psi_1$ gives us

$$\dot{a}(\psi_1+O(\varepsilon))=c\psi_1+\varepsilon P\begin{pmatrix}\mathcal{T}_{-a}\mathcal{G}(\xi\mathcal{T}_a u^*,\mathcal{T}_a u^*,x,0)\\0\end{pmatrix}+\varepsilon P\begin{pmatrix}q\\0\end{pmatrix}.$$

Projecting onto ψ_1 gives

$$\dot{a}(\langle\psi_1,\psi_1\rangle(1+O(\varepsilon))) = c\langle\psi_1,\psi_1\rangle + \varepsilon\left\langle\begin{pmatrix}\mathcal{T}_{-a(t)}\mathcal{G}(\xi\mathcal{T}_a u^*,\mathcal{T}_a u^*,x,0)\\0\end{pmatrix},\psi_1\right\rangle + \varepsilon\left\langle\begin{pmatrix}q\\0\end{pmatrix},\psi_1\right\rangle.$$

Since ε and c are assumed to be small we can neglect the higher order terms that appear as a result of dividing by $1+O(\varepsilon)$. Letting

$$r(a) = -\frac{\left\langle\begin{pmatrix}\mathcal{T}_{-a}\mathcal{G}(\xi\mathcal{T}_a u^*,\mathcal{T}_a u^*,x,0)\\0\end{pmatrix},\psi_1\right\rangle}{\langle\psi_1,\psi_1\rangle}, \tag{3.5.5}$$

$$\hat{q} = \frac{\left\langle\begin{pmatrix}q\\0\end{pmatrix},\psi_1\right\rangle}{\langle\psi_1,\psi_1\rangle},$$

we get the system of differential equations

$$\begin{aligned} a_t &= c - \varepsilon r(a) + \varepsilon\hat{q}(a,c,\varepsilon),\\ c_t &= 0, \end{aligned}$$

where $\hat{q}(a,c,\varepsilon)\to 0$ uniformly as $(\varepsilon,c)\to(0,0)$. □

An application of the implicit function theorem tells us that for (ε,c) close enough to $(0,0)$ there exists a curve of equilibria such that $a_t = 0$. This curve is the graph of the function $c = \varepsilon r(a)+\varepsilon\sigma(a,\varepsilon)$ where σ is some bounded function with the property $\sigma(a,0)=0$ [11, 16]. Thus, it follows that if

$$\inf_{a\in\mathbb{R}}\{r(a)+\sigma(a,\varepsilon)\} < \frac{c}{\varepsilon} < \sup_{a\in\mathbb{R}}\{r(a)+\sigma(a,\varepsilon)\} \tag{3.5.6}$$

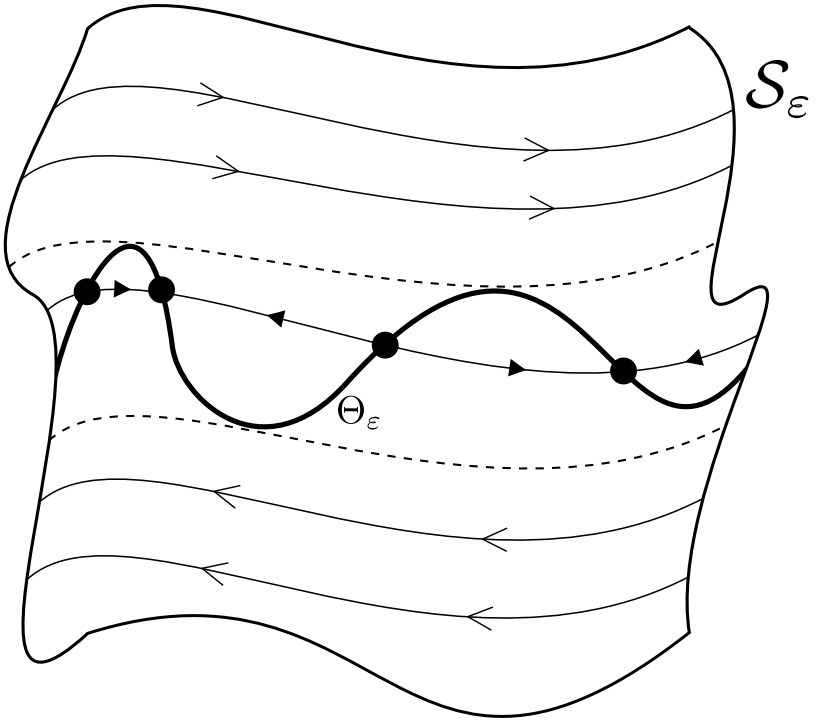

Figure 3.2: The perturbed equilibrium on the manifold $\mathcal{S}_\varepsilon$. The curve Θ_ε corresponds to the set of blocking points and is given by $a_t = 0$. ([11] Figure 3 p. 26).

then at some point between $a \in \mathbb{R}$ we expect $a_t = 0$. This means that, at some point in time, the travelling front will reach an equilibrium point at which the wave is stationary. In other words the wave is blocked.

We remark that for (ε, c) close enough to $(0, 0)$ the term $\sigma(a, \varepsilon)$ becomes negligible. Hence, close to $(0, 0)$, the parameter region where we expect propagation failure is approximated by $\inf_{a\in\mathbb{R}}\{r(a)\}$ and $\sup_{a\in\mathbb{R}}\{r(a)\}$.

Theorem 3.5.2. *Consider the nonlinear differential equation on a Banach space X*

$$u_t = \mathcal{A}u + \mathcal{F}(u, \alpha) + \varepsilon\mathcal{G}(\xi u, u, x; \varepsilon) \tag{3.5.7}$$

which generates a local semi flow on the corresponding Banach space Y. Suppose that $\mathcal{A}$ and ξ are linear operators whose domains are dense in Y and is such that there is an Γ-invariant subspace on which all operators commute. Furthermore, suppose

that hypotheses 3.1.2, 3.2.1, 3.3.1 and 3.4.1 are satisfied. Then, for all $0 \leq \varepsilon \ll 1$ *the semiflow admits a smooth stable invariant manifold* $\mathcal{S}_\varepsilon$*. Solutions of* (3.5.7) *that belong to* $\mathcal{S}_\varepsilon$ *correspond to perturbed relative equilibria with non-constant speed. In this case, wave blocking occurs in a cone in the* (c, ε) *parameter space characterized by the inequality*

$$\inf_{a\in\mathbb{R}}\{r(a)\} < \frac{c}{\varepsilon} < \sup_{a\in\mathbb{R}}\{r(a)\}. \tag{3.5.8}$$

where $r(a)$ *is the same as in proposition 3.5.1.*

The wedge defined by inequality (3.5.8) is illustrated in Figure 3.3.

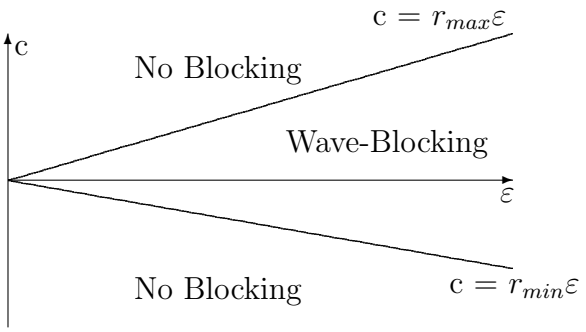

Figure 3.3: Wave-blocking occurs for values of (ε, c) inside the wedge. Here r_{max} and r_{min} are the supremum and infimum of (3.5.8) respectively.

Chapter 4

Numerical Results

4.1 Numerical Setup

In this chapter, we show the implications of theorem 3.5.2 using specific examples of perturbations. In doing so we return to the well-studied bistable equation

$$\frac{\partial u}{\partial t} = \frac{\partial^2 u}{\partial x^2} + u(1-u)(u-\alpha),$$

which admits a travelling wave solution that can be derived analytically. The resulting wave profile is given by

$$u^*(x) = \frac{1}{2}\left(1 + \tanh\left(\frac{x}{2\sqrt{2}}\right)\right).$$

In order to effectively compare the results of our theory, we need to find the inf/sup of the function $r(a)$ given by (3.5.5). We start by computing $\langle \psi_1, \psi_1 \rangle$.

$$\begin{aligned}
\langle \psi_1, \psi_1 \rangle &= \int_{\mathbb{R}} \xi u^* \cdot \xi u^* dx \\
&= \int_{\mathbb{R}} \frac{1}{32} \operatorname{sech}^4\left(\frac{x}{2\sqrt{2}}\right) dx \\
&= \frac{\sqrt{2}}{12}.
\end{aligned}$$

In order to proceed further we need to specify the form of the perturbation $\mathcal{G}$. However, deriving an analytical expression for the numerator in (3.5.5) is not always feasible. Thus, we need to choose an efficient numerical scheme that will allow us to find $r(a)$ and subsequently determine the associated inequality (3.5.8).

In order to find the supremum and infimum of $r(a)$ we need only consider the values of a in the interval $[-A, A]$, A sufficiently large. We can do this because all perturbations in the preceding section will be periodic with period l. Since $\mathcal{G}$ and u^* are bounded and ξu^* is localized, we need only integrate over a sufficiently large interval. Thus, for each fixed a we will use Simpsons rule on the interval $x \in [-100, 100]$ to determine the corresponding value of $r(a)$. This procedure will yield a good approximation to the maximum/minimum provided we choose an sufficiently small step size for our discretization.

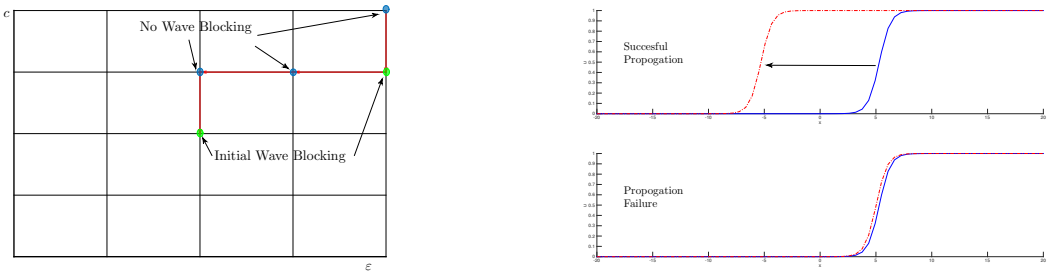

Figure 4.1: A visualization of the scheme used to numerically obtain the initial blocking values.

The numerical scheme described above allows us to approximate the wave blocking wedge defined by theorem 3.5.2. In order to test our result we need to implement a secondary numerical scheme to obtain the observed wave blocking values (See Figure 4.1). First, the (ε, c) parameter space is discretized into a set of points (c_i, ε_j). Next, for each point (c_i, ε_j), we numerically solve equation (1.1.5) for $t \in [0, t_f]$ with an translation of u^* as the initial condition. For each fixed ε_j the initial blocking values are determined by searching for some value of c for which the wave failed to

advance. This is done, with fixed decimal precision, by comparing the difference between $u(0,x)$ and $u(t_f,x)$, t_f sufficiently large. The curve of initial values determined through this procedure are compared with the corresponding approximations for the supremum and infimum of $r(a)$.

4.2 Example 1: Perturbation In The Reaction Term

Here we consider a perturbation in the intrinsic growth parameter. We would like to take $\rho = \rho(x)$ to be a periodic step function similar to that shown in Figure 1.1. However, doing so would not guarantee the smoothness of the perturbation $\mathcal{G}$ required in hypothesis 3.1.2. Thus, to fix this problem we begin by considering the function $p(x) = \cos^n(x)$ where n is any odd integer. Then

$$\begin{aligned} P(x) = \int \cos^n(x)\,dx &= \int \frac{1}{2^{n-1}} \sum_{k=0}^{(n-1)/2} \binom{n}{k} \cos((n-2k)x)\,dx \\ &= \frac{1}{2^{n-1}} \sum_{k=0}^{(n-1)/2} \binom{n}{k} \int \cos((n-2k)x)\,dx \\ &= \frac{1}{2^{n-1}} \sum_{k=0}^{(n-1)/2} \binom{n}{k} \frac{\sin((n-2k)x)}{n-2k}. \end{aligned}$$

The function $P(x)$ numerically behaves like a periodic step function and is sufficiently smooth allowing us to apply our main result to (see Figure 4.2). Thus, we take ρ to be $\rho(x) = 1 + \varepsilon\frac{P(x)}{A}$ where $A = \max\{P(x)\}$. For our purposes we take $n = 3$ to get

$$\rho(x) = 1 + \varepsilon\left(\frac{9}{8}\sin(x) + \frac{1}{8}\sin(3x)\right).$$

Thus, the RDE

$$\frac{\partial u}{\partial t} = \frac{\partial^2 u}{\partial x^2} + \rho(x)u(1-u)(u-\alpha)$$

can be written in the form (3.1.1) with

$$\mathcal{G}(u_x, u, x; \varepsilon) = \left(\frac{9}{8}\sin(x) + \frac{1}{8}\sin(3x)\right) u(1-u)(u-\alpha). \tag{4.2.1}$$

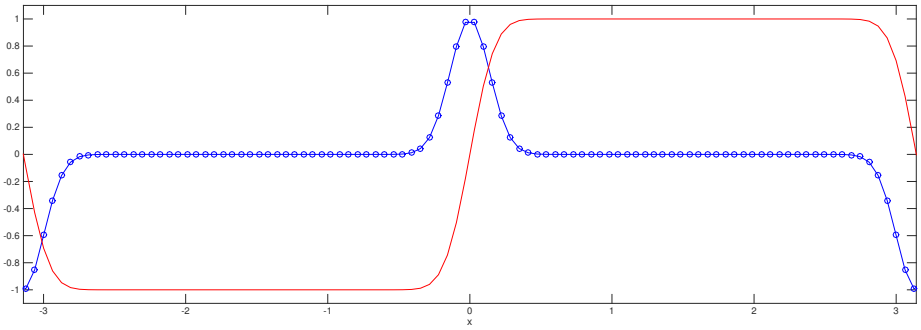

Figure 4.2: Plot of $p(x)$ (solid blue line with circles) and $P(x)$ (solid red line) with $n = 13$.

Applying the numerical integration scheme previously described, we are able to generate a graphical representation of $r(a)$ (see Figure 4.3). We also find that $\sup\{r(a)\} \approx 0.1765$ and $\inf\{r(a)\} \approx -0.1765$. Thus, our theoretical approach suggests that wave-blocking occurs inside a wedge defined by $-0.1765 < \frac{c}{\varepsilon} < 0.1765$. A comparison between our theoretically obtained values and numerically obtained values is given in Figure 4.4.

4.3 Example 2: Perturbation In The Diffusion Term

Studying the effects of non-constant diffusion on the speed of propagation was one of the motivating factors for extending the work done by Roy and LeBlanc [11, 16]. Here we consider the reaction-diffusion equation

$$\frac{\partial u}{\partial t} = \frac{\partial}{\partial x}\left[D(x)\frac{\partial u}{\partial x}\right] + u(1-u)(u-\alpha). \tag{4.3.1}$$

In order to keep our problem analytically tractable, we consider $D(x) = 1 - \varepsilon\sin(x)$ and apply theorem 3.5.2. We introduce a change of variables $x = y + \varepsilon\zeta(y)$ to

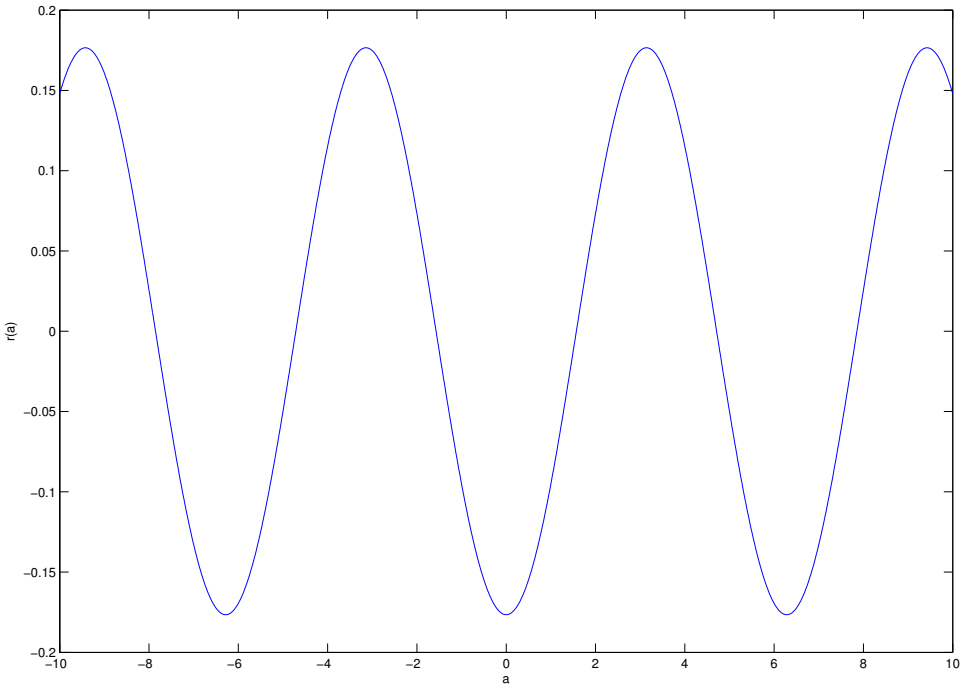

Figure 4.3: Plot of $r(a)$ for $\mathcal{G}$ given by (4.2.1).

transform (4.3.1) into an equation of the form (3.1.1). Doing so gives

$$\frac{\partial u}{\partial t} = \frac{1-\varepsilon\sin(y+\varepsilon\zeta(y))}{(1+\varepsilon\zeta'(y))^2}\frac{\partial^2 u}{\partial y^2} - \frac{\varepsilon\cos(y+\varepsilon\zeta(y))}{1+\varepsilon\zeta'(y)}\frac{\partial u}{\partial y} - \frac{\varepsilon\zeta''(y)(1-\varepsilon\sin(y+\varepsilon\zeta(y))}{(1+\varepsilon\zeta'(y))^3}\frac{\partial u}{\partial y} + u(1-u)(u-\alpha).$$

We choose the function $\zeta(y)$ such that it satisfies the differential equation

$$\frac{1-\varepsilon\sin(y+\varepsilon\zeta(y))}{(1+\varepsilon\zeta'(y))^2} = 1 \tag{4.3.2}$$

and is such that $\varepsilon\zeta(y) \to 0$ as $\varepsilon \to 0$. This change of variables now gives us the RDE

$$u_t = u_{yy} + u(1-u)(u-\alpha) + \varepsilon g(u_y, u, x, \varepsilon)$$

where

$$g(u_y, u, x, \varepsilon) = -\frac{\cos(y+\varepsilon\zeta(y))}{1+\varepsilon\zeta'(y)}\frac{\partial u}{\partial y} - \frac{\zeta''(y)(1-\varepsilon\sin(y+\varepsilon\zeta(y))}{(1+\varepsilon\zeta'(y))^3}\frac{\partial u}{\partial y}.$$

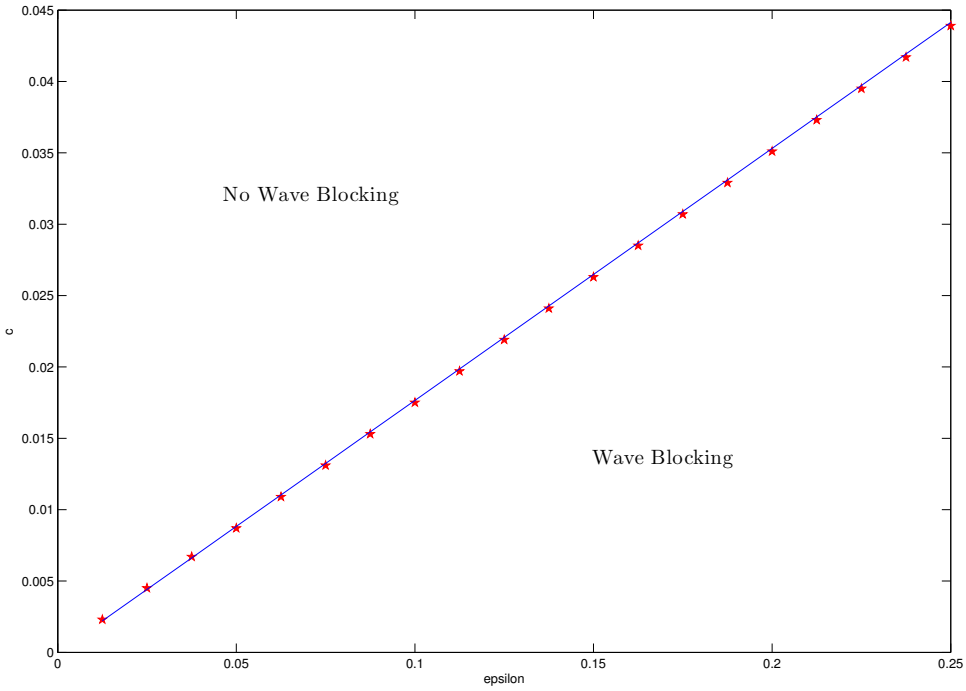

Figure 4.4: Comparison between the blocking wedge (line) and the numerically calculated values of wave-blocking (stars) for the perturbation corresponding to (4.2.1)

Using the identities

$$\begin{aligned} y + \varepsilon\zeta(y)\big|_{\varepsilon=0} &= y, \\ 1 + \varepsilon\zeta'(y)\big|_{\varepsilon=0} &= 1, \\ \zeta''(y)\big|_{\varepsilon=0} &= -\frac{1}{2}\cos(y) \end{aligned}$$

we get

$$r(a) = -\frac{6}{\sqrt{2}} \int_{-\infty}^{\infty} \cos(y-a) u_y^* \cdot \xi u^* dy.$$

Applying the same numerical approach as before, we find that $\sup\{r(a)\} \approx 0.15679$ and $\inf\{r(a)\} \approx -0.15679$. Thus, our theorem predicts that the wave will block if

$-0.15679\varepsilon \leq c \leq 0.15679\varepsilon$. We compare our prediction with that of our numerical simulation. The results are illustrated in Figure 4.5.

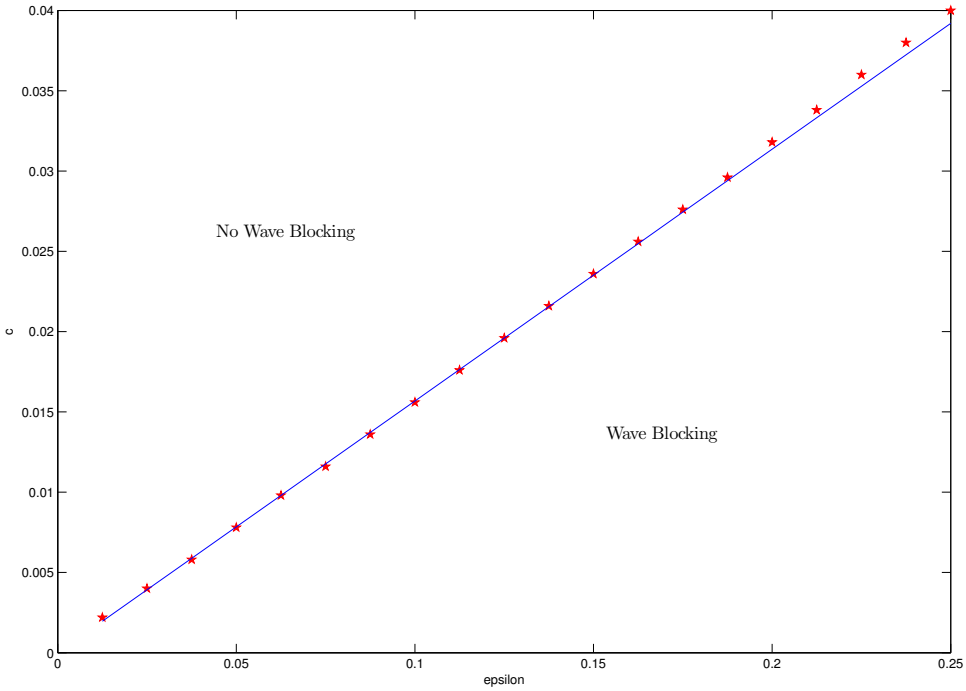

Figure 4.5: Comparison between the blocking wedge (line) and the numerically calculated values of wave-blocking (stars) for (4.3.1).

4.4 Example 3: Ecological Diffusion

We modify equation (4.3.1) and consider

$$\frac{\partial u}{\partial t} = \frac{\partial^2}{\partial x^2}\left[\mu(x)u\right] + u(1-u)(u-\alpha). \tag{4.4.1}$$

This modification represents ecological diffusion and accomodates for spatial variability in motility, predicting that individuals eventually accumulate in desirable habitats and avoid undesirable areas (see section 4.5 for more details). Ecological diffusion is

appropriate when organisms make local decisions regarding movement, rather than nonlocal decisions as in the Fickian case [2, 20].

Here we take $\mu(x) = 1 - \varepsilon\sin(x)$. As in the previous example we introduce a change of variables $x = y + \varepsilon\zeta(y)$ so as to transform (4.4.1) into an equation of the form (3.1.1). Substituting the change of variables into (4.4.1) gives

$$\begin{aligned}\frac{\partial u}{\partial t} &= \frac{1-\varepsilon\sin(y+\varepsilon\zeta(y))}{(1+\varepsilon\zeta'(y))^2}\frac{\partial^2 u}{\partial y^2} \\ &\quad + \left(-\frac{2\varepsilon\cos(y+\varepsilon\zeta(y))}{1+\varepsilon\zeta'(y)} - \frac{\varepsilon\zeta''(y)(1-\varepsilon\sin(y+\varepsilon\zeta(y)))}{(1+\varepsilon\zeta'(y))^3}\right)\frac{\partial u}{\partial y} \\ &\quad + \varepsilon\sin(y+\varepsilon\zeta(y))u + u(1-u)(u-\alpha).\end{aligned}$$

Setting the coefficient of $\frac{\partial^2 u}{\partial y^2}$ to 1 we find that $\zeta(y)$ must solve the differential equation given by (4.3.2). When $\varepsilon = 0$ we find the arrive at the identities

$$\begin{aligned} y + \varepsilon\zeta(y)\big|_{\varepsilon=0} &= y, \\ 1 + \varepsilon\zeta'(y)\big|_{\varepsilon=0} &= 1, \\ \zeta''(y)\big|_{\varepsilon=0} &= -\frac{1}{2}\cos(y)\end{aligned}$$

which were the same as in the previous example. Thus, we get

$$r(a) = -\frac{12}{\sqrt{2}}\int_{-\infty}^{\infty}(\sin(y-a)u^* - \frac{3}{2}\cos(y-a)u_y^*)\cdot\xi u^* dy.$$

Integrating numerically, we find that $\max\{r(a)\} \approx 0.47037$ and $\min\{r(a)\} \approx -0.47037$. So we expect wave-blocking to occur in a wedge defined by $c = 0.47037\varepsilon$ and $c = -0.47037\varepsilon$. We compare our prediction with that of our numerical simulation. The results are illustrated in Figure 4.6. Unlike the previous two examples, when $\varepsilon > 0.1$ our numerical results begins to diverge from our theoretical prediction. This is because our theory provides a linear approximation to the wedge. Thus, for this model, the nonlinear terms in (3.5.6) are no longer negligible for $\varepsilon > 0.1$.

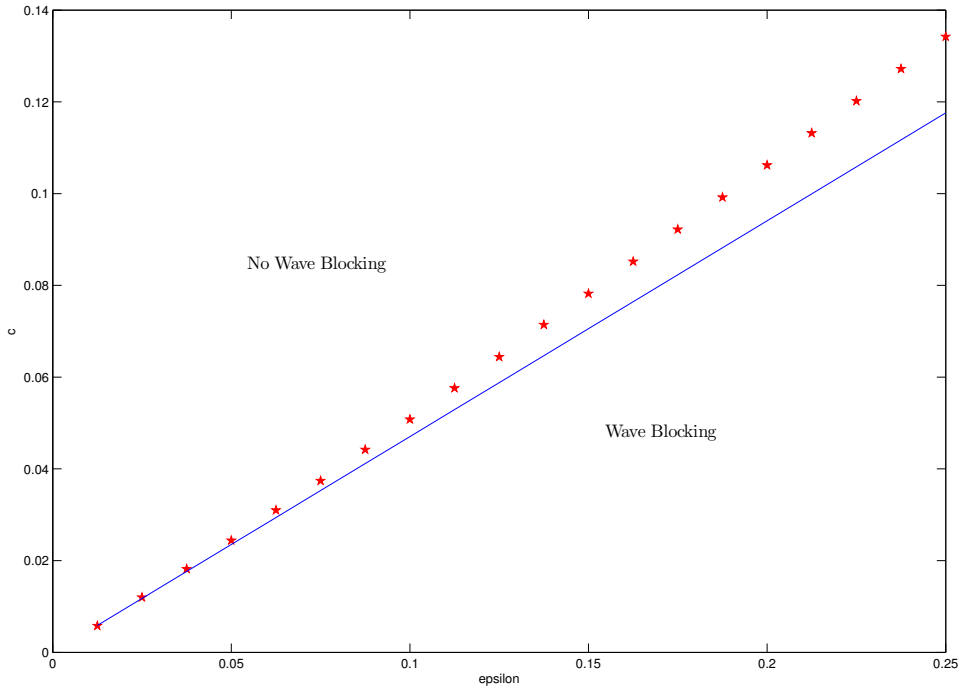

Figure 4.6: Comparison between the blocking wedge (line) and the numerically calculated values of wave-blocking (stars) for the perturbation in (4.4.1).

4.5 Example 4: Spatial Correlation

In the previous examples, we considered perturbations in either the reaction or the diffusion term. However, ecologically spatial perturbations are more likely to impact both terms. Let's reconsider both the classical Fickian diffusion and ecological diffusion models with the same perturbation in the reaction term. The Fickian diffusion models will take the form

$$\frac{\partial u}{\partial t} = \frac{\partial}{\partial x}\left[D(x)\frac{\partial u}{\partial x}\right] + \rho(x)u(1-u)(u-\alpha). \tag{4.5.1}$$

and our second model is

$$\frac{\partial u}{\partial t} = \frac{\partial^2}{\partial x^2}\left[\mu(x)u\right] + \rho(x)u(1-u)(u-\alpha). \tag{4.5.2}$$

were $\mu(x) = D(x) = 1-\varepsilon\sin(x)$ and $\rho(x) = 1+\varepsilon\sin(x-\boldsymbol{\theta})$. The parameter $\boldsymbol{\theta} \in [0, 2\pi]$ is the phase difference between μ, D and ρ. If $\boldsymbol{\theta} \neq \pi$ then we say that the parameters are out of phase.

As we did in examples 2 and 3, we need to define an appropriate change of variables such that equations (4.5.1) and (4.5.2) can be transformed into an equation of the form (3.1.1). Utilizing the same transformation from the previous two examples we do get an equation to which we can apply our main theorem. Numerically integrating as we have done in the previous sections, we are able to plot the maximum of $r(a)$ as a function of $\boldsymbol{\theta}$. The results are illustrated in Figure 4.7. Figure 4.7 provides a great deal of insight into how the parameter $\boldsymbol{\theta}$ impacts the slope of the wave blocking wedge for both models.

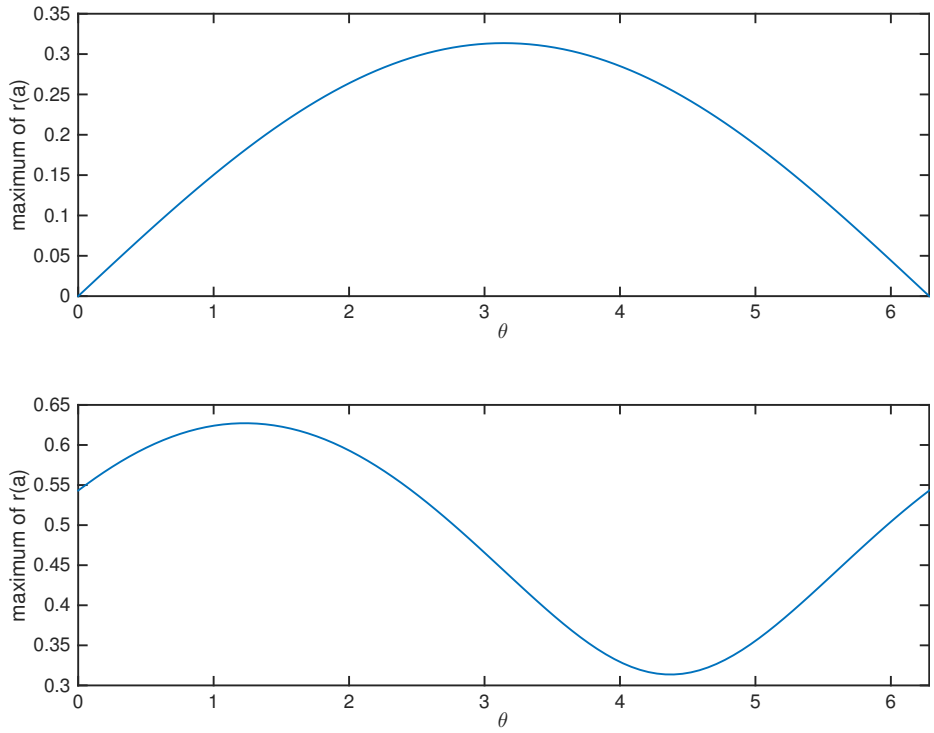

Figure 4.7: Plot of $\sup\{r(a)\}$ as a function of $\boldsymbol{\theta}$ for equation (4.5.1) (Top) and (4.5.2) (Bottom).

For the classical model (4.5.1) the results are as we would expect; when individu-

als slow down in an area where there is a decrease in the intrinsic growth rate then it becomes harder to overcome the Allee threshold and so we expect to see propagation failure or invasion pinning. In order for this to occur we need both ρ and D to be in phase, i.e. we need $\boldsymbol{\theta} = \pi$. From our plot we can see that when $\boldsymbol{\theta} = \pi$ the slope of the wedge is at its maximum meaning that small perturbations have a higher likely hood of causing wave blocking.

One major difference in the two plots in Figure 4.7 is the scale of the vertical axis. For equation (4.5.1) we have $r_{max} \in [0, 0.35]$ and for equation (4.5.2) we have $r_{max} \in [0.3, 0.65]$. In order to understand the difference in the scale, we must step away from our model and examine movement in a heterogeneous environment.

Let us assume that our organisms are moving on a lattice of spatial positions. The organism may take a step of length Δx to the right with probability $R(t, x)$, to the left with probability $L(t, x)$ or make no movement at all with probability $N(t, x)$. Thus, an organism at any location x could only come from one of three possible locations; $x - \Delta x$, x or $x + \Delta x$. If $p(t, x)$ is the probability of finding the organism at the spatial location x for any time t then [20]

$$\begin{aligned} p(t,x) = N(t-\Delta t, x)p(t-\Delta t, x) + R(t-\Delta t, x-\Delta x)p(t-\Delta t, x-\Delta x) \\ + L(t-\Delta t, x+\Delta x)p(t-\Delta t, x+\Delta x). \end{aligned}$$

Using the appropriate Taylor series expansions and then gathering similar terms Turchin [20] showed that

$$\frac{\partial p}{\partial t} \approx \frac{\partial^2}{\partial x^2}\left[\frac{(\Delta x)^2(R+L)}{2\Delta t}p\right] - \frac{\partial}{\partial x}\left[\frac{\Delta x(R-L)}{\Delta t}p\right]. \tag{4.5.3}$$

We assume that $R - L = O(\Delta x)$ and we choose the limit of $\Delta x, \Delta t \to 0$ in such a way that $(\Delta x)^2/\Delta t$ converges to a finite number. Thus, taking the limit $\Delta x, \Delta t \to 0$ in equation (4.5.3) leads to

$$\frac{\partial p}{\partial t} = \frac{\partial^2}{\partial x^2}(\mu p) - \frac{\partial}{\partial x}(\beta p),$$

where

$$\mu = \lim_{(\Delta t,\Delta x)\to(0,0)} \frac{(\Delta x)^2(R+L)}{2\Delta t} \qquad \text{and} \qquad \beta = \lim_{(\Delta t,\Delta x)\to(0,0)} \frac{\Delta x(R-L)}{\Delta t}.$$

Here μ defines the motility and β defines the movement bias. The movement bias is proportional to the difference between the probability of moving to the right versus moving to the left. Both β and μ appear inside the partial derivatives because, in general, they are functions of space and time [20].

Returning to our model, we rewrite the diffusion term in (4.5.1) as

$$\frac{\partial}{\partial x}\left[D(x)\frac{\partial u}{\partial x}\right] = \frac{\partial^2}{\partial x^2}\left[D(x)u\right] - \frac{\partial}{\partial x}\left[D'(x)u\right].$$

We now observe that D defines motility, which is proportional to the probability of moving, while D' defines the movement bias. If $D' < 0$ then the population has a movement bias to the left and when $D' > 0$ there is a bias to move to the right (see Figure 4.8) [20].

When $\boldsymbol{\theta} = 0$ or 2π individuals experience a movement bias towards areas with high motility but low growth. This is an ecologically advantageous strategy in the presence of an strong Allee effect. In order for the population to successfully spread it must first overcome the corresponding Allee threshold. This is an easier task when individuals choose to work together instead of "going it alone". Thus, it is easier for the species to overcome the perturbation and spread.

In contrast, when $\boldsymbol{\theta} = \pi$, individuals experience a movement bias towards areas with high motility and high growth. The problem this presents is that individuals favour "going it alone" in areas of low growth. This makes it harder to overcome the Allee threshold. Thus, small perturbations are more likely to cause wave blocking than if we had chosen a different value of $\boldsymbol{\theta}$.

We note that equation (4.5.2) does not include a movement bias. Therefore, individuals have equal probability of moving to the left and to the right. As a result, overcoming the Allee threshold becomes a more difficult task. Thus, any spatial

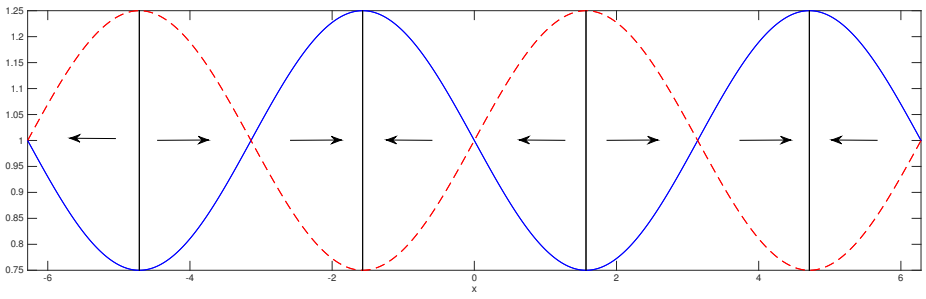

Figure 4.8: Plot of $\rho(x)$ (dashed red line) and $D(x)$ (solid blue line) for $\varepsilon = 0.25$ and $\boldsymbol{\theta} = 0$. The arrows indicate the direction of the movement bias.

perturbation in motility and growth is more likely to cause wave blocking than in the case of equation (4.5.1). In fact, Figure 4.7 implies that the species will favour a lag between $\rho(x)$ and $D(x)$.

Chapter 5

Conclusion

In this thesis, we studied the phenomenon of wave blocking in the context of reaction diffusion equations, focusing on the relationship between non-constant diffusion and the speed of propagation. As such, we built upon the work of LeBlanc and Roy [11, 16], extending their work to perturbations which included the first partial derivative. Their ideas allowed us to develop an approach that let us find a wedge in the (c, ε) parameter space that defines when wave blocking will occur. The most simple model that we tested was the bistable equation (1.1.5). This model allowed us to verify our hypothesis and perform most computations explicitly.

The techniques presented here and by LeBlanc and Roy [11, 16] are derived by utilizing the translational symmetry of the underlying, unperturbed problem. To that extent, we formulated a hypothesis on the symmetry of the reaction term $\mathcal{F}$ and the asymmetry of the function $\mathcal{G}$. Furthermore, we asked that the unperturbed system be parameterized by the wave speed in such a way that when $(c, \varepsilon) = (0, 0)$ our system admitted a stationary steady state.

The spectral gap condition of LeBlanc and Roy [11, 16] which ensured the persistence of solutions under light perturbations. From there, we reduced the dynamics of our system to a finite dimensional manifold and studied the line of equilibria corre-

sponding to $c = 0$. When $\varepsilon \neq 0$ this line of equilibria persisted but was deformed on the perturbed manifold. It is this perturbed line of equilibria that causes propagation failure when (c, ε) lies in the cone emanating from $(0, 0)$ in the (c, ε) parameter space. Our main result is summarized in theorem 3.5.2.

We have shown the implications of theorem 3.5.2 using specific examples of perturbations. This was done by comparing the blocking wedge predicted by our theory with values of blocking obtained through numerical simulations. We observed that, for small values of ε, the theoretical and numerical approaches yield almost the exact same result. In contrast, as ε gets larger we find that our theory begins to loose precision. This is due to the fact that the nonlinear terms in the inequality (3.5.6) begin to have a larger contribution in determining the blocking threshold. This is readily seen in section 4.3 where we considered perturbed ecological diffusion (see Figure 4.6).

Moving forward, there are two paths along which to proceed. The first is to show that this theory can be extended to systems of RDEs. It is often the case that multiple species live in the same habitat and that they interact with each other. The relationships in which these species exist can be cooperative or competitive. Extending our theory to these systems of equations would provide us with greater insight into the relationship between habitat fragmentation and interspecies cooperation/-competition. However, in systems, it can be difficult to get an exact expression for the unperturbed wave. As a consequence of this, deriving and verifying analogous statements to those presented in this thesis could be an arduous task.

Another path stems from the observation that translational symmetry is intertwined with the phenomena of travelling waves. In higher spatial dimensions we can observe other types of symmetries such as rotational symmetry. This work has only addressed what we would expect in one spatial dimension. Given the diversity in symmetries in higher dimensions, we are left wondering how wave blocking may be affected in these higher dimensions. For example, the region in the parameter space

that causes wave blocking may depend on the strength of the heterogeneity but also on the spatial arrangement of the perturbation. Ecologically, we would want to ask what spatial arrangement of habitats minimizes/maximizes the region in parameter space that leads to invasion pinning.

Appendix A

MATLAB Code

Here we provide the MATLAB codes used in chapter 4. There are two sets of codes included here. The first is based upon the numerical approach described in chapter 4 to numerically determine the function $r(a)$. The second set of codes is numerical program designed to solve equation (3.5.7) and numerically determine the cone of wave-blocking parameters. Running these programs for various different perturbations we are able to compare our theoretical predictions against the numerically obtained values.

A.1 Numerical Calculation of $r(a)$

```
%% Theoretical Calculation of r(a)
% this file plots the function r(a) while calculating the
% maximum and minimum values.
close; clear; clc
format long g

%% Define the interval of integration
```

```
xlo=-100;    xhi=100;    dx=0.05;
n=(xhi-xlo)/dx;
xx=xlo:dx:xhi;

%% Define the interval for which r(a) is defined
alo=-100;    ahi=100;    da = 0.05;
N=(ahi-alo)/da;

%% Calculate, numerically, r(a)
for i=0:N
    A(i+1)=alo+da*i;
    L = 2*sqrt(2);

    %Define the profile of the travelling wave
    u = @(x) 0.5*(1+ tanh(x/L));

    %Derivative of the wave profile
    du = @(x) (sqrt(2)/8)*(1-tanh(x/L).*tanh(x/L));

    %Define the Purturbation function G
    G = @(x) [(9/8)*sin(x-A(i+1)) + (1/8)*sin(3*(x-A(i+1)))
        ].* u(x).*(1-u(x)).*(u(x)-0.5);

    %Define the integrand
    f = @(x) G(x).*du(x);

    %Calculate the value of r(a) using simpsons rule
```

```
    R(i+1)= dx/3*(f(xx(1))+2*sum(f(xx(3:2:end-2)))+4*sum(f(xx
        (2:2:end)))+f(xx(end)));
    R(i+1) = -(12/sqrt(2))*R(i+1);
end
fprintf('\n Maximum = %f \n', max(R))
fprintf('\n Minimum = %f \n', min(R))
figure(1); plot(A,R); xlabel('a') ;ylabel('r(a)')
```

A.2 Wedge Plotting Program

```
%% Wave Blocking Wedge Plots
% This file numerically determines the region in the
    parameter space that
% leads to wave blocking. It does this by solving the given
    PDE and then
% tracking the evolution of the solution in time. The program
     solves the
% PDE continuously until it finds a parameter combination for
     which
%                    u(0,x) - u(tfinal,x)< 0.05
% where x is fixed. This program uses MATLABs PDE solver
    PDEPE. The
% relevant function files can be found at the end of the
    script.

clear; close; clc
global epsil alpha
```

```
%% Define the solution mesh
t0=0;   tfinal=2000;   x=linspace(-75,75,500);   t=t0:tfinal;

%% PDEPE Parameters
warning off MATLAB:fzero:UndeterminedSyntax
m=0; cstep=0.0002; rmax =0.1765;



for qq=0:19
    epsil = 0.25*(20-qq)/20;
    if qq ==0
        c=0.05;
    elseif qq>0
        c = C(qq);
    end
    BLOCK=0;
    while BLOCK==0
    alpha = 0.5*(1-sqrt(2)*c);
        %% Solving the PDE
        u = pdepe(m,@mypde,@initial,@bc1,x,t);
        if u(tfinal+1,251)<0.05
            BLOCK=1;
            C(qq+1)=c;
            TC(qq+1)=epsil*rmax;
            EE(qq+1)=epsil;
        else c=c-cstep;
        end;
```

```
    end
end

figure(1);
    hold all
    plot(EE,C,'ro',EE,TC,'b-'); xlabel('epsilon'); ylabel('c'
        );

%% Define the initial condition
function initial = initial(x)
    global epsil alpha
    initial = 0.5*(1+tanh((x-10)/(2*sqrt(2))));

%% Define the boundary Conditions
function [pl,ql,pr,qr] = bc1(xl,ul,xr,ur,t)
    pl=ul; ql=0; pr=ur-1; qr=0;

%% Define the PDE
function [c,b,s] = mypde(x,t,u,DuDx)
    global epsil alpha
    c=1;
    b = DuDx;
    s = (1+epsil*[ (9/8)*sin(x) + (1/8)*sin(3*x)] )*u*(1-u)*(
        u-alpha);
```

Bibliography

[1] F. Courchamp, L. Berec, and J. Gascoigne. *Allee Effects in Ecology and Conservation*. Oxford University Press, 1 edition, 2008.

[2] M. Garlick, J. Powell, M. Hooten, and L. McFarlane. Homogenization of large-scale movement models in ecology. *Bulletin of Mathematical Biology*, 73(9):2088–2108, Jan 2011.

[3] D. Henry. *Geometric Theory of Semilinear Parabolic Equations*. Number 804 in Lecture Notes in Mathematics. Springer-Verlag, New York, 1981.

[4] J. Keener. Homogenization and propagation in the bistable equation. *Physica D: Nonlinear Phenomena*, 136(1):1–17, 2000.

[5] J. Keener and T. Lewis. Wave-blocking in excitable media due to regions of depressed excitability. *SIAM Journal on Applied Mathematics*, 61(1):293–316, 2000.

[6] J. Keener and J. Sneyd. *Mathematical Physiology*. Springer, New York, 2009.

[7] T. Keitt, M. A. Lewis, and R. Holt. Allee effects, invasion pinning, and species' borders. *The American Naturalist*, 157(2):203–216, February 2001.

[8] N. Kinezaki, K. Kawasaki, and N. Shigesada. Spatial dynamics of invasion in sinusoidally varying environments. *Population Ecology*, 48(4):263–270, April 2006.

[9] N. Kinezaki, K. Kawasaki, F. Takasu, and N. Shigesada. Modeling biological invasions into periodically fragmented environments. *Theoretical Population Biology*, 64(3):291–302, 2003.

[10] G. Lajoie. Wave blocking phenomenon : a dynamical systems approach. Master's thesis, University of Ottawa, 2007.

[11] V. LeBlanc and C. Roy. Forced translational symmetry-breaking for abstract evolution equations. *Journal of Abstract Differential Equations and Applications*, 4(2):16–43, 2013.

[12] M. A. Lewis and P. Kareiva. Allee dynamics and the spread of invading organisms. *Theoretical Population Biology*, 43(2):141–158, April 1993.

[13] G. Maciel and F. Lutscher. Allee effects and population spread in patchy landscapes. *Journal of Biological Dynamics*, 9(1):109–123, December 2015.

[14] J. Musgrave, F. Lutscher, and A. Girard. Population spread in patchy landscapes under a strong allee effect. *Theoretical Ecology*, January 2015.

[15] H. Othmer. A continuum model for coupled cells. *Journal of Mathematical Biology*, 17:351–369, 1983.

[16] C. Roy. The origin of wave blocking for a bistable reaction-diusion equation : A general approach. Master's thesis, University of Ottawa, 2012.

[17] B. Sandstede, A. Scheel, and C. Wulff. Dynamics of spiral waves on unbounded domains using center-manifold reductions. *Journal of Differential Equations*, 141(1):122–149, November 1997.

[18] N. Shigesada, K. Kawasaki, and E. Teramoto. Traveling periodic waves in heterogeneous environments. *Theoretical Population Biology*, 30:143–160, 1986.

[19] P. Tobin, S. Whitmire, D. Johnson, O. Bjornstad, and M. Liebhold. Invasion speed is affected by geographical variation in the strength of allee effects. *Ecology Letters*, 10:36–43, 2007.

[20] P. Turchin. *Quantitative Analysis of Movement*. Sinauer Associates, 1998.

[21] A. I. Volpert, V.A. Volpert, and V.A. Volpert. *Travelling Wave Solutions of Parabolic Systems*, volume 140 of *Translation of Mathematical Monographs*. American Mathematical Society, Providence, R.I., 1994.